Siberian Branch of Russian Academy of Science
BUDKER INSTITUTE OF NUCLEAR PHYSICS

A.B. Arbuzov, G.V. Fedotovich, F.V. Ignatov,
E.A. Kuraev, A.L. Sibidanov

MONTE-CARLO GENERATOR FOR THE PROCESSES $e^+e^- \to e^+e^-$, $\mu^+\mu^-$, $\pi^+\pi^-$ and K^+K^-, K_LK_S WITH PRECISE RADIATIVE CORRECTIONS AT LOW ENERGIES

Budker INP 2004-70

Novosibirsk
2004

Monte-Carlo generator for the processes $e^+e^- \to e^+e^-$, $\mu^+\mu^-$, $\pi^+\pi^-$ and K^+K^-, K_LK_S with precise radiative corrections at low energies

A.B. Arbuzov[1], *G.V. Fedotovich*[2], *F.V. Ignatov*[2], *E.A. Kuraev*[1], *A.L. Sibidanov*[2]

[1] Bogoliubov Laboratory of Theoretical Physics, JINR, Dubna, 141980, Russia

[2] Budker Institute of Nuclear Physics, Novosibirsk, 630090, RF

Abstract

The cross sections of e^+e^- annihilation into hadrons were measured with CMD-2 detector at VEPP-2M collider in the energy range from 0.37 to 1.39 GeV with the systematic uncertainty about 0.6%. Monte Carlo Generator with Photon Jets (MCGPJ) was created to simulate Bhabha scattering events, production of two charged pions (kaons) and muons. Radiative corrections (RC) in the first order of α are taken into account exactly. By means of structure function formalism the leading logarithmic contributions with photon jets emission in collinear region are calculated in higher orders. Changes in kinematics due to collinear jets emission are preserved. The theoretical cross sections accuracy with RC is estimated to be better than $\sim 0.2\%$. The numerous tests of the program, comparison with other MC generators and CMD-2 experimental data are presented.

1 Introduction

Experimental studies of e^+e^- annihilation into hadrons at low energies are very important in various problems of particle physics. The recent measurement of the muon anomalous magnetic moment

$$a_\mu = (g-2)_\mu/2$$

at BNL [1] led to a new world average, differing by 2.6 standard deviation from its theoretical evaluation [3]. One of the main ingredients in the theoretical prediction for a_μ is the hadronic vacuum polarization contribution related via a dispersion integral with the cross section of e^+e^- annihilation into hadrons. The ratio

$$R(s) = \sigma(e^+e^- \to \text{hadrons})/\sigma(e^+e^- \to \mu^+\mu^-)$$

is dominated by the $e^+e^- \to \pi^+\pi^-$ channel at low energies. In the case of a_μ the energy range covered by the VEPP-2M collider gives the major contribution both to the hadronic vacuum polarization contribution itself and to its uncertainty [2].

This uncertainty is mainly driven by the systematic and statistical errors of the experimental values of $R(s)$ which one has to use as an input to the integral with the proper kernel function [4]:

$$a_\mu^{had} = \left(\frac{\alpha m_\mu}{3\pi}\right)^2 \int\limits_{4m_\pi^2}^{\infty} \frac{R(s)K(s)}{s^2}\mathrm{d}s.$$

As for high energy region, $\sqrt{s} > 10$ GeV, this integral can be evaluated within the perturbative QCD framework. A numerical value of this integral approximately is equal to ~ 70 ppm [3].

The aim of the new BNL experiment [5] is to measure the muon anomalous magnetic moment with the relative accuracy ~ 0.25 ppm in order to improve the previous result [1] by a factor of two. To calculate with the same accuracy the hadronic contribution to the value a_μ^{had}, the required theoretical precision of the cross sections with radiative corrections (RC) has to be achieved with the accuracy better than 0.3% (70ppm $\times 0.3\% \sim 0.2$ ppm).

The detection efficiency, background conditions, kinematic distributions differ for specific e^+e^- annihilation modes. Therefore different selection criteria are required to extract events from the raw data. So the expressions for the cross sections with RC must have a completely differential form with respect to the kinematic variables. In this case the influence of the selection criteria as well as the detector resolution and trigger efficiency can be naturally incorporated in MC generator.

In this paper we describe the MCGPJ generator which simulates processes $e^+e^- \to e^+e^-$, $\mu^+\mu^-$, $\pi^+\pi^-$, K^+K^- and K_LK_S. The accuracy of the formulae for the cross sections is estimated to be about 0.2% [6, 7]. As it will be shown below this precision mainly determines the systematic error of the integrated luminosity as well as the systematic error of the hadronic cross sections.

The vacuum polarization effects in the virtual photon propagator are treated as in Ref [6] for the lepton channels. These effects are not included in RC for the hadronic modes according to the generally accepted agreement [8]. In this case the cross section value at a resonance peak directly determines the leptonic width.

The radiatively corrected cross sections for annihilation channels with accuracy about 0.1% were obtained in [9]. Unfortunately, expressions for these cross sections do not contain the angular distributions for the emitted photons and, as a result, it is not possible to reconstruct the kinematics of final particles correctly. The differential cross sections were derived in [10], but their relative accuracy is about 1%, since only $\mathcal{O}(\alpha)$ corrections were taken into account.

The considerable efforts were devoted to elucidate the theoretical understanding of the cross section accuracy with RC, especially for the case of low energy e^+e^- and $\pi^+\pi^-$ pairs production. The work [6] is based in part on a combination of the approaches of the two last papers mentioned above. To achieve the accuracy 0.2% higher order corrections were taken into account by means of the Structure Function (SF) formalism [9]. It involves a convolution of the *shifted* Born cross section with the electron (positron) Structure Function - $\mathcal{D}(x,s)$. SF describes the leading effects due to emission photon jets in collinear region as well as e^+e^- pairs radiation off the incoming and out coming electron and positron. These enhanced contributions are proportional to $(\alpha/\pi)^n \ln^n(s/m_e^2)$, where $n = 1, 2, ...$ and are referred to as leading ones. Moreover, in the *smoothed* representations of the SF [9] a certain part of the corrections is exponentiated and evaluated in all orders in α. The first order non-leading terms proportional to (α/π) are embedded in RC exactly. The next-to-leading terms of the second order, $(\alpha/\pi)^2 \ln(s/m_e^2) \sim 0.01\%$,

are fortunately small and can be omitted, keeping in mind the present precision tag. The emission of one hard photon at large angles is described by a differential formula, which allows to take into account specific experimental conditions and cuts.

The MCGPJ code is the MC generator for Bhabha scattering events and it is described in detail below. A generator for production of muons, pions, charge and neutral kaons is also presented. The program has a modular structure that simplifies the implementation of additional hadronic modes as well as the replacement of matrix elements of the current cross sections by a new one. The effects of the final state radiation (FSR) for the channels $\mu^+\mu^-, \pi^+\pi^-, K^+K^-$ have been incorporated into the program. The pions were assumed to be point-like, and scalar QED was applied to calculate virtual, soft and hard photon emission by charged pions (kaons).

2 Monte-Carlo generator for events Bhabha scattering at large angles

The *shifted* Born cross section of the process

$$e^-(z_1 p_-) + e^+(z_2 p_+) \to e^-(p_1) + e^+(p_2)$$

corrected by vacuum polarization factors in s and t channels, when initial particles lose some energy by radiation of photon jets in collinear region, has a well known form [6] in the center-of-mass system and reads as

$$\frac{\mathrm{d}\tilde{\sigma}_0^{e^+e^-\to e^+e^-}(z_1,z_2)}{\mathrm{d}\Omega_1} = \frac{4z_1z_2\alpha^2}{a^2\tilde{s}}\left(\frac{\tilde{s}^2+\tilde{u}^2}{2\tilde{t}^2|1-\Pi(\tilde{t})|^2} + \frac{\tilde{t}^2+\tilde{u}^2}{2\tilde{s}^2|1-\Pi(\tilde{s})|^2} + \Re\mathrm{e}\left\{\frac{\tilde{u}^2}{\tilde{s}\tilde{t}}\frac{1}{(1-\Pi(\tilde{s}))(1-\Pi(\tilde{t}))}\right\}\right), \quad (1)$$

where z_1 and z_2 are the electron and positron reduced energies after photon jets radiation ($z_{1,2} = \varepsilon_{1,2}/\varepsilon_{beam}$), $\Pi(\tilde{s})$ and $\Pi(\tilde{t})$ - vacuum polarization operators in the virtual photon propagators in s and t channels, respectively. The Mandelstam variables in the Lab and c.m.s. are defined as usual:

$$s = 2p_-p_+, \qquad t = -2p_-p_1, \qquad u = -2p_-p_2,$$
$$\tilde{s} = sz_1z_2, \quad \tilde{t} = -sz_1Y_1\frac{1-c_1}{2}, \quad \tilde{u} = -sz_2Y_1\frac{1+c_1}{2},$$

where $c_1 = \cos\theta_1$, θ_1 is a polar angle between direction of the electron motion and the electron beam direction, Y_1 and Y_2 are the reduced energies of

final particles. The energy-momentum conservation laws allow to find these energies and the positron polar angle θ_2:
$z_1 + z_2 = Y_1 + Y_2$ is the energy conservation law,
$z_1 - z_2 = Y_1 \cos\theta_1 + Y_2 \cos\theta_2$ is the momentum conservation law along Z-axis,
$Y_1 \sin\theta_1 = Y_2 \sin\theta_2$ is the momentum conservation law in the plane perpendicular to the Z-axis. From these equations one can find

$$Y_1 = \frac{2z_1 z_2}{a}, \qquad Y_2 = \frac{(z_1^2 + z_2^2) - (z_1^2 - z_2^2)c_1}{a},$$
$$c_2 = \frac{(z_1^2 - z_2^2) - (z_1^2 + z_2^2)c_1}{(z_1^2 + z_2^2) - (z_1^2 - z_2^2)c_1}, \quad \text{where } a = z_1 + z_2 - (z_1 - z_2)c_1. \quad (2)$$

In order to calculate the cross section using simulated events, the crucial point is to construct the final particles kinematics as close as possible to the real events when RC are embedded in the MC generator. The expression for the differentional cross section with one hard photon emission in the reaction,

$$e^-(p_-) + e^+(p_+) \to e^-(p_1) + e^+(p_2) + \gamma(k),$$

was obtained in Ref. [10] (see references therein) and reads

$$\mathrm{d}\sigma_{\mathrm{hard}} = \frac{\alpha^3}{2\pi^2 s} R^{e^+e^-\to e^+e^-\gamma} \mathrm{d}\Gamma, \quad (3)$$

where $\mathrm{d}\Gamma$ is a phase-space volume of the three final particles:

$$\mathrm{d}\Gamma = \frac{\mathrm{d}^3p_1}{\varepsilon_1}\frac{\mathrm{d}^3p_2}{\varepsilon_2}\frac{\mathrm{d}^3k}{\omega}\delta^{(4)}(p_- + p_+ - p_1 - p_2 - k), \quad (4)$$

where ε_1, ε_2, and ω are the energies of the final state electron, positron and photon, respectively; δ-function provides the energy-momentum conservation.

The expression for the $R^{e^+e^-\to e^+e^-\gamma}$ dealing with vacuum polarization effects in photon propagators was derived in paper [6] and it is given by:

$$R^{e^+e^-\to e^+e^-\gamma} = \frac{(WT)_\Pi}{4} \quad (5)$$
$$-\frac{m_e^2}{\chi_+'^2}\left(\frac{s^2 + (s+t)^2}{2t^2(1-\Pi(t))^2} + \frac{t^2 + (s+t)^2}{2s^2|1-\Pi(s)|^2} + \Re\mathrm{e}\left\{\frac{(s+t)^2}{st(1-\Pi(s))(1-\Pi(t))}\right\}\right)$$
$$-\frac{m_e^2}{\chi_-'^2}\left(\frac{s^2 + (s+t_1)^2}{2t_1^2(1-\Pi(t_1))^2} + \frac{t_1^2 + (s+t_1)^2}{2s^2|1-\Pi(s)|^2} + \Re\mathrm{e}\left\{\frac{(s+t_1)^2}{st_1(1-\Pi(s))(1-\Pi(t_1))}\right\}\right)$$

$$-\frac{m_e^2}{\chi_+^2}\left(\frac{s_1^2+(s_1+t)^2}{2t^2(1-\Pi(t))^2}+\frac{t^2+(s_1+t)^2}{2s_1^2|1-\Pi(s_1)|^2}+\Re\mathrm{e}\left\{\frac{(s_1+t)^2}{s_1t(1-\Pi(s_1))(1-\Pi(t))}\right\}\right)$$
$$-\frac{m_e^2}{\chi_-^2}\left(\frac{s_1^2+(s_1+t_1)^2}{2t_1^2(1-\Pi(t_1))^2}+\frac{t_1^2+(s_1+t_1)^2}{2s_1^2|1-\Pi(s_1)|^2}+\Re\mathrm{e}\left\{\frac{(s_1+t_1)^2}{s_1t_1(1-\Pi(s_1))(1-\Pi(t_1))}\right\}\right),$$

where the invariants and $\chi_\pm$, $\chi'_\pm$ are defined as: $s=2p_-p_+$, $s_1=2p_1p_2$, $t=-2p_-p_1$, $t_1=-2p_+p_2$, $\chi_\pm=kp_\pm$, $\chi'_\pm=kp_{1,2}$. $(WT)_\Pi$ describes the process with one hard photon emission outside the collinear region [6] and reads

$$\begin{aligned}(WT)_\Pi &= \frac{SS}{|1-\Pi(s)|^2s\chi'_-\chi'_+}+\frac{S_1S_1}{|1-\Pi(s_1)|^2s_1\chi_-\chi_+}-\frac{TT}{|1-\Pi(t)|^2t\chi_+\chi'_+}\\
&-\frac{T_1T_1}{|1-\Pi(t_1)|^2t_1\chi_-\chi'_-}+\Re\mathrm{e}\left[\frac{TT_1}{(1-\Pi(t))(1-\Pi(t_1))tt_1\chi_-\chi'_-\chi_+\chi'_+}\right.\\
&-\frac{SS_1}{(1-\Pi(s))(1-\Pi(s_1))^*ss_1\chi_-\chi'_-\chi_+\chi'_+}+\frac{TS}{(1-\Pi(t))(1-\Pi(s))ts\chi'_-\chi_+\chi'_+}\\
&+\frac{T_1S_1}{(1-\Pi(t_1))(1-\Pi(s_1))t_1s_1\chi_-\chi'_-\chi_+}-\frac{T_1S}{(1-\Pi(t_1))(1-\Pi(s))t_1s\chi_-\chi'_-\chi'_+}\\
&\left.-\frac{TS_1}{(1-\Pi(\tilde{t}))(1-\Pi(\tilde{s}_1))ts_1\chi_-\chi_+\chi'_+}\right], \qquad (6)\end{aligned}$$

where the following notations are used:

$$\begin{aligned}SS &= S_1S_1=t^2+t_1^2+u^2+u_1^2,\\
TT &= T_1T_1=s^2+s_1^2+u^2+u_1^2,\\
SS_1 &= (t^2+t_1^2+u^2+u_1^2)\times(t\chi_+\chi'_++t_1\chi_-\chi'_--u\chi_+\chi'_--u_1\chi_-\chi'_+),\\
TT_1 &= (s^2+s_1^2+u^2+u_1^2)\times(u\chi_+\chi'_-+u_1\chi_-\chi'_++s\chi'_-\chi'_++s_1\chi_-\chi_+),\\
TS &= -\frac{1}{2}(u^2+u_1^2)(s(t+s_1)+t(s+t_1)-uu_1),\\
TS_1 &= -\frac{1}{2}(u^2+u_1^2)(t(s_1+t_1)+s_1(s+t)-uu_1),\\
T_1S &= \frac{1}{2}(u^2+u_1^2)(t_1(s+t)+s(s_1+t_1)-uu_1),\\
T_1S_1 &= \frac{1}{2}(u^2+u_1^2)(s_1(s+t_1)+t_1(s_1+t)-uu_1). \qquad (7)\end{aligned}$$

The main contribution to the cross section with photon radiation comes from the collinear region where the cross section exhibits a very steep behavior. Therefore it is necessary to consider it carefully as it was done in

Ref. [11]. The collinear region is a part of the angular phase-space with four narrow cones surrounding the directions of motion of the initial and final charged particles. The emitted photon should be inside these cones with an open angle $2\theta_0$. The angle θ_0 should obey the restrictions, $1/\gamma \ll \theta_0 \ll 1$ ($\gamma = \varepsilon_{beam}/m_e$). It serves as an auxiliary parameter, but in certain situation it can be related with the experimental angular resolution of the detector. Usually its value is taken about $\sim 1/\sqrt{\gamma}$.

The cross section integrated inside these narrow cones takes the form [6]:

$$\frac{\mathrm{d}\sigma_{\mathrm{coll}}^{ee\to ee+\gamma}}{\mathrm{d}\Omega_1} = \frac{\alpha}{\pi}\int\limits_{\Delta}^{1}\frac{\mathrm{d}x}{x}\left\{2\,\frac{\mathrm{d}\tilde{\sigma}_0(1,1)}{\mathrm{d}\Omega_1}\left[\left(z+\frac{x^2}{2}\right)\left(L-1+\ln\frac{\theta_0^2 z^2}{4}\right)+\frac{x^2}{2}\right]\right.$$
$$\left.+\left[\frac{\mathrm{d}\tilde{\sigma}_0(z,1)}{\mathrm{d}\Omega_1}+\frac{\mathrm{d}\tilde{\sigma}_0(1,z)}{\mathrm{d}\Omega_1}\right]\left[\left(z+\frac{x^2}{2}\right)\left(L-1+\ln\frac{\theta_0^2}{4}\right)+\frac{x^2}{2}\right]\right\}, \qquad (8)$$

where $L = \ln(s/m_e^2)$, $z = 1-x$ and the *shifted* Born cross section is defined in Eq. (1). The auxiliary parameter $\Delta = \Delta\varepsilon/\varepsilon$ ($\Delta \ll 1$) serves as a separator of hard and soft photons, where ε is the beam energy. The terms proportional to $(\alpha/\pi)(L-1)$ are contained in SF [9] and therefore should be removed from this expression. The remaining four terms can be interpreted as the four so-called *compensators*. One can see below the remarkable phenomena - these *compensators* provide independence of the total cross section with respect to the auxiliary parameter θ_0 when they are summed with the last term in Eq. (9). It allows to superpose exactly the cross section with one hard photon inside and outside narrow cones.

The formalism dealing with the SF approach provides the essential accuracy improvement of the Bhabha cross section calculation by taken into account the radiation of photon jets in collinear regions. Let us enumerate these improvements:

- the photon jets radiation (enhanced contributions) is taken into account by means SF formalism;
- to combine the cross sections with radiation of one hard photon inside and outside narrow cones the four *compensators* are embedded into the *master* formula (Eq. 9);
- the *shifted* Born cross section contributes to the total one according to the SF weights in (Eq. 9);
- the vacuum polarization effects are inserted in all photon propagators exactly;

- the expression for one hard photon emission is decomposed into three parts which represents initial and final state radiation as well as their interference;
- the non-leading contribution of the first order of α, proportional to the Born cross section is taken into account by so-called *K-factor*.

The *master* formula, discribing e^+e^- production can be found in paper [6] and it is given by

$$
\begin{aligned}
\frac{\mathrm{d}\sigma^{e^+e^-\to e^+e^-(n\gamma)}}{\mathrm{d}\Omega_1} &= \int_0^1 \mathrm{d}x_1 \int_0^1 \mathrm{d}x_2 \int_0^1 \mathrm{d}x_3 \int_0^1 \mathrm{d}x_4 \frac{\mathrm{d}\tilde{\sigma}_0(z_1,z_2)}{\mathrm{d}\Omega_1} \\
&\times \mathcal{D}(z_1,s)\mathcal{D}(z_2,s)\mathcal{D}(z_3,\tilde{s})\mathcal{D}(z_4,\tilde{s}) \left(1+\frac{\alpha}{\pi}\tilde{K}_{SV}\right)\Theta(\text{cuts}) \\
&+\frac{\alpha}{\pi}\int_\Delta^1 \frac{\mathrm{d}x_1}{x_1}\left[\left(z_1+\frac{x_1^2}{2}\right)\ln\frac{\theta_0^2}{4}+\frac{x_1^2}{2}\right]\frac{\mathrm{d}\tilde{\sigma}_0(z_1,1)}{\mathrm{d}\Omega_1}\Theta(\text{cuts}) \\
&+\frac{\alpha}{\pi}\int_\Delta^1 \frac{\mathrm{d}x_2}{x_2}\left[\left(z_2+\frac{x_2^2}{2}\right)\ln\frac{\theta_0^2}{4}+\frac{x_2^2}{2}\right]\frac{\mathrm{d}\tilde{\sigma}_0(1,z_2)}{\mathrm{d}\Omega_1}\Theta(\text{cuts}) \\
&+\frac{\alpha}{\pi}\int_\Delta^1 \frac{\mathrm{d}x_3}{x_3}\left[\left(z_3+\frac{x_3^2}{2}\right)\ln\frac{\theta_0^2 z_3^2}{4}+\frac{x_3^2}{2}\right]\frac{\mathrm{d}\tilde{\sigma}_0(1,1)}{\mathrm{d}\Omega_1}\Theta(\text{cuts}) \\
&+\frac{\alpha}{\pi}\int_\Delta^1 \frac{\mathrm{d}x_4}{x_4}\left[\left(z_4+\frac{x_4^2}{2}\right)\ln\frac{\theta_0^2 z_4^2}{4}+\frac{x_4^2}{2}\right]\frac{\mathrm{d}\tilde{\sigma}_0(1,1)}{\mathrm{d}\Omega_1}\Theta(\text{cuts}) \\
&+\frac{4\alpha}{\pi}\frac{\mathrm{d}\tilde{\sigma}_0(1,1)}{\mathrm{d}\Omega_1}\ln\frac{u}{t}\ln\Delta+\frac{\alpha^3}{2\pi^2 s}\int\limits_{\substack{k^0>\Delta\varepsilon\\ \theta_\gamma>\theta_0}}\frac{(WT)_\Pi}{4}\frac{\mathrm{d}\Gamma}{\mathrm{d}\Omega_1}\Theta(\text{cuts}), \qquad (9)
\end{aligned}
$$

where $x_{1,2.3,4}$ are the relative energies emitted photon jets along motion of the initial and final particles; $z_{1,2,3,4} = 1 - x_{1,2,3,4}$ are the energy fractions of the initial and final particles after photon jets radiation; $\Theta(\text{cuts})$ is a Θ-function equal to 1 or 0 if the kinematics variables meet the demands or not

selection criteria (cuts); $\tilde{K}_{SV}(\tilde{\theta}_1)$ is defined in Ref. [10, 6] and it is:

$$\tilde{K}_{SV}(\tilde{\theta}_1) = -1 - 2\mathrm{Li}_2(\sin^2\frac{\tilde{\theta}_1}{2}) + 2\mathrm{Li}_2(\cos^2\frac{\tilde{\theta}_1}{2}) + \frac{1}{(3+\tilde{c}_1^2)^2}\cdot$$
$$\Big[\frac{\pi^2}{3}(2\tilde{c}_1^4 - 3\tilde{c}_1^3 - 15\tilde{c}_1) + 2(2\tilde{c}_1^4 - 3\tilde{c}_1^3 + 9\tilde{c}_1^2 + 3\tilde{c}_1 + 21)\ln^2(\sin\frac{\tilde{\theta}_1}{2})$$
$$-4(\tilde{c}_1^4 + \tilde{c}_1^2 - 2\tilde{c}_1)\ln^2(\cos\frac{\tilde{\theta}_1}{2}) - 4(\tilde{c}_1^3 + 4\tilde{c}_1^2 + 5\tilde{c}_1 + 6)\ln^2(\tan\frac{\tilde{\theta}_1}{2}) +$$
$$2(\tilde{c}_1^3 - 3\tilde{c}_1^2 + 7\tilde{c}_1 - 5)\ln(\cos\frac{\tilde{\theta}_1}{2}) + 2(3\tilde{c}_1^3 + 9\tilde{c}_1^2 + 5\tilde{c}_1 + 31)\ln(\sin\frac{\tilde{\theta}_1}{2})\Big],$$

where electron scattering angle should be taken in c.m.s. The cosine of this angle according to Lorenz transformation is equal to:

$$\tilde{c}_1 = [-(z_1 - z_2) + (z_1 + z_2)c_1]/a.$$

The integration limits in each integral of the first term in Eq. (9) were divided in two parts from 0 to Δ and from Δ to the maximal jet energy. As a result, the four-fold integral splits into sixteen separate parts. Those of them with one photon jet radiation are merged in a proper way with *compensators* in the *master* formula.

The first contribution takes into account the effects due to soft and virtual radiative corrections and it is given by

$$\frac{\mathrm{d}\sigma_1^{e^+e^-\to e^+e^-(n\gamma)}}{\mathrm{d}\Omega_1} = \int_0^\Delta\int_0^\Delta\int_0^\Delta\int_0^\Delta \mathrm{d}x_1\mathrm{d}x_2\mathrm{d}x_3\mathrm{d}x_4\mathcal{D}(z_1,s)\mathcal{D}(z_2,s)\mathcal{D}(z_3,\tilde{s})$$
$$\times\mathcal{D}(z_4,\tilde{s})\big(1+\frac{\alpha}{\pi}\tilde{K}_{SV}\big)\frac{\mathrm{d}\tilde{\sigma}_0(z_1,z_2)}{\mathrm{d}\Omega_1} - \frac{4\alpha}{\pi}\ln\Big(\frac{u}{t}\Big)\ln\Delta\frac{\mathrm{d}\tilde{\sigma}_0(1,1)}{\mathrm{d}\Omega_1}. \quad (10)$$

The photon jets emitted by each charged particles can have energy up to $\Delta\varepsilon$. This part also contains the contribution due to production of virtual and soft real e^+e^- pairs if $2m_e < \Delta\varepsilon$.

The next four terms represent contribution to the cross section with emission of one hard jet along motion of any charged particles, supplied with the virtual and soft leading logarithmic corrections of the remaining *legs*. The relevant *compensators* are included. The jet energy is greater than $\Delta\varepsilon$ and

its maximal value is defined by energy-momentum conservation.

$$\frac{\mathrm{d}\sigma_2^{e^+e^-\to e^+e^-+n\gamma}}{\mathrm{d}\Omega_1} = \int\limits_{\Delta}^{1}\int\limits_{0}^{\Delta}\int\limits_{0}^{\Delta}\int\limits_{0}^{\Delta} \mathrm{d}x_1\mathrm{d}x_2\mathrm{d}x_3\mathrm{d}x_4 \mathcal{D}(z_2,s)\mathcal{D}(z_3,\tilde{s})\mathcal{D}(z_4,\tilde{s})$$
$$\times\left[\mathcal{D}(z_1,s)\big(1+\frac{\alpha}{\pi}\tilde{K}_{SV}\big)+\frac{\alpha}{\pi}\frac{1}{x_1}\left(\big(z_1+\frac{x_1^2}{2}\big)\ln\frac{\theta_0^2}{4}+\frac{x_1^2}{2}\right)\right]$$
$$\times\frac{\mathrm{d}\tilde{\sigma}_0(z_1,z_2)}{\mathrm{d}\Omega_1}\Theta(\text{cuts}), \tag{11}$$

$$\frac{\mathrm{d}\sigma_3^{e^+e^-\to e^+e^-+n\gamma}}{\mathrm{d}\Omega_1} = \int\limits_{0}^{\Delta}\int\limits_{\Delta}^{1}\int\limits_{0}^{\Delta}\int\limits_{0}^{\Delta} \mathrm{d}x_1\mathrm{d}x_2\mathrm{d}x_3\mathrm{d}x_4 \mathcal{D}(z_1,s)\mathcal{D}(z_3,\tilde{s})\mathcal{D}(z_4,\tilde{s})$$
$$\times\left[\mathcal{D}(z_2,s)\big(1+\frac{\alpha}{\pi}\tilde{K}_{SV}\big)+\frac{\alpha}{\pi}\frac{1}{x_2}\left(\big(z_2+\frac{x_2^2}{2}\big)\ln\frac{\theta_0^2}{4}+\frac{x_2^2}{2}\right)\right]$$
$$\times\frac{\mathrm{d}\tilde{\sigma}_0(z_1,z_2)}{\mathrm{d}\Omega_1}\Theta(\text{cuts}), \tag{12}$$

$$\frac{\mathrm{d}\sigma_4^{e^+e^-\to e^+e^-+n\gamma}}{\mathrm{d}\Omega_1} = \int\limits_{0}^{\Delta}\int\limits_{0}^{\Delta}\int\limits_{\Delta}^{1}\int\limits_{0}^{\Delta} \mathrm{d}x_1\mathrm{d}x_2\mathrm{d}x_3\mathrm{d}x_4 \mathcal{D}(z_1,s)\mathcal{D}(z_2,s)\mathcal{D}(z_4,\tilde{s})$$
$$\times\left[\mathcal{D}(z_3,\tilde{s})\big(1+\frac{\alpha}{\pi}\tilde{K}_{SV}\big)+\frac{\alpha}{\pi}\frac{1}{x_3}\left(\big(z_3+\frac{x_3^2}{2}\big)\ln\frac{\theta_0^2 z_3^2}{4}+\frac{x_3^2}{2}\right)\right]$$
$$\times\frac{\mathrm{d}\tilde{\sigma}_0(z_1,z_2)}{\mathrm{d}\Omega_1}\Theta(\text{cuts}), \tag{13}$$

$$\frac{\mathrm{d}\sigma_5^{e^+e^-\to e^+e^-+n\gamma}}{\mathrm{d}\Omega_1} = \int\limits_{0}^{\Delta}\int\limits_{0}^{\Delta}\int\limits_{0}^{\Delta}\int\limits_{\Delta}^{1} \mathrm{d}x_1\mathrm{d}x_2\mathrm{d}x_3\mathrm{d}x_4 \mathcal{D}(z_1,s)\mathcal{D}(z_2,s)\mathcal{D}(z_3,\tilde{s})$$
$$\times\left[\mathcal{D}(z_4,\tilde{s})\big(1+\frac{\alpha}{\pi}\tilde{K}_{SV}\big)+\frac{\alpha}{\pi}\frac{1}{x_4}\left(\big(z_4+\frac{x_4^2}{2}\big)\ln\frac{\theta_0^2 z_4^2}{4}+\frac{x_4^2}{2}\right)\right]$$
$$\times\frac{\mathrm{d}\tilde{\sigma}_0(z_1,z_2)}{\mathrm{d}\Omega_1}\Theta(\text{cuts}). \tag{14}$$

The next six terms represent the contribution to the cross section with emission of two jets along momenta of any two charged particles. The both

jet energies are greater than $\Delta\varepsilon$ and their maximal values are defined by the energy-momentum conservation.

$$\frac{\mathrm{d}\sigma_6^{e^+e^-\to e^+e^-+n\gamma}}{\mathrm{d}\Omega_1} = \int\limits_{\Delta}^{1}\int\limits_{\Delta}^{1}\int\limits_{0}^{\Delta}\int\limits_{0}^{\Delta}\mathrm{d}x_1\mathrm{d}x_2\mathrm{d}x_3\mathrm{d}x_4\mathcal{D}(z_1,s)\mathcal{D}(z_2,s)\mathcal{D}(z_3,\tilde{s})\mathcal{D}(z_4,\tilde{s}) \times\frac{\mathrm{d}\tilde{\sigma}_0(z_1,z_2)}{\mathrm{d}\Omega_1}\left(1+\frac{\alpha}{\pi}\tilde{K}_{SV}\right)\Theta(\text{cuts}), \tag{15}$$

$$\frac{\mathrm{d}\sigma_7^{e^+e^-\to e^+e^-+n\gamma}}{\mathrm{d}\Omega_1} = \int\limits_{\Delta}^{1}\int\limits_{0}^{\Delta}\int\limits_{\Delta}^{1}\int\limits_{0}^{\Delta}\mathrm{d}x_1\mathrm{d}x_2\mathrm{d}x_3\mathrm{d}x_4\mathcal{D}(z_1,s)\mathcal{D}(z_2,s)\mathcal{D}(z_3,\tilde{s})\mathcal{D}(z_4,\tilde{s}) \times\frac{\mathrm{d}\tilde{\sigma}_0(z_1,z_2)}{\mathrm{d}\Omega_1}\left(1+\frac{\alpha}{\pi}\tilde{K}_{SV}\right)\Theta(\text{cuts}), \tag{16}$$

$$\frac{\mathrm{d}\sigma_8^{e^+e^-\to e^+e^-+n\gamma}}{\mathrm{d}\Omega_1} = \int\limits_{\Delta}^{1}\int\limits_{0}^{\Delta}\int\limits_{0}^{\Delta}\int\limits_{\Delta}^{1}\mathrm{d}x_1\mathrm{d}x_2\mathrm{d}x_3\mathrm{d}x_4\mathcal{D}(z_1,s)\mathcal{D}(z_2,s)\mathcal{D}(z_3,\tilde{s})\mathcal{D}(z_4,\tilde{s}) \times\frac{\mathrm{d}\tilde{\sigma}_0(z_1,z_2)}{\mathrm{d}\Omega_1}\left(1+\frac{\alpha}{\pi}\tilde{K}_{SV}\right)\Theta(\text{cuts}), \tag{17}$$

$$\frac{\mathrm{d}\sigma_9^{e^+e^-\to e^+e^-+n\gamma}}{\mathrm{d}\Omega_1} = \int\limits_{0}^{\Delta}\int\limits_{\Delta}^{1}\int\limits_{\Delta}^{1}\int\limits_{0}^{\Delta}\mathrm{d}x_1\mathrm{d}x_2\mathrm{d}x_3\mathrm{d}x_4\mathcal{D}(z_1,s)\mathcal{D}(z_2,s)\mathcal{D}(z_3,\tilde{s})\mathcal{D}(z_4,\tilde{s}) \times\frac{\mathrm{d}\tilde{\sigma}_0(z_1,z_2)}{\mathrm{d}\Omega_1}\left(1+\frac{\alpha}{\pi}\tilde{K}_{SV}\right)\Theta(\text{cuts}), \tag{18}$$

$$\frac{\mathrm{d}\sigma_{10}^{e^+e^-\to e^+e^-+n\gamma}}{\mathrm{d}\Omega_1} = \int\limits_{0}^{\Delta}\int\limits_{\Delta}^{1}\int\limits_{0}^{\Delta}\int\limits_{\Delta}^{1}\mathrm{d}x_1\mathrm{d}x_2\mathrm{d}x_3\mathrm{d}x_4\mathcal{D}(z_1,s)\mathcal{D}(z_2,s)\mathcal{D}(z_3,\tilde{s})\mathcal{D}(z_4,\tilde{s}) \times\frac{\mathrm{d}\tilde{\sigma}_0(z_1,z_2)}{\mathrm{d}\Omega_1}\left(1+\frac{\alpha}{\pi}\tilde{K}_{SV}\right)\Theta(\text{cuts}), \tag{19}$$

$$\frac{\mathrm{d}\sigma_{11}^{e^+e^-\to e^+e^-+n\gamma}}{\mathrm{d}\Omega_1} = \int\limits_{0}^{\Delta}\int\limits_{0}^{\Delta}\int\limits_{\Delta}^{1}\int\limits_{\Delta}^{1}\mathrm{d}x_1\mathrm{d}x_2\mathrm{d}x_3\mathrm{d}x_4\mathcal{D}(z_1,s)\mathcal{D}(z_2,s)\mathcal{D}(z_3,\tilde{s})\mathcal{D}(z_4,\tilde{s}) \times\frac{\mathrm{d}\tilde{\sigma}_0(z_1,z_2)}{\mathrm{d}\Omega_1}\left(1+\frac{\alpha}{\pi}\tilde{K}_{SV}\right)\Theta(\text{cuts}). \tag{20}$$

The following four terms represent contribution to the cross section with emission of three jets along momenta of any three charged particles. The jet energies are greater than $\Delta\varepsilon$ and their maximal values are defined again by the energy-momentum conservation.

$$\frac{\mathrm{d}\sigma_{12}^{e^+e^-\to e^+e^-+n\gamma}}{\mathrm{d}\Omega_1} = \int\limits_{\Delta}^{1}\int\limits_{\Delta}^{1}\int\limits_{\Delta}^{1}\int\limits_{0}^{\Delta}\mathrm{d}x_1\mathrm{d}x_2\mathrm{d}x_3\mathrm{d}x_4\mathcal{D}(z_1,s)\mathcal{D}(z_2,s)\mathcal{D}(z_3,\tilde{s})\mathcal{D}(z_4,\tilde{s}) \times\frac{\mathrm{d}\tilde{\sigma}_0(z_1,z_2)}{\mathrm{d}\Omega_1}\left(1+\frac{\alpha}{\pi}\tilde{K}_{SV}\right)\Theta(\text{cuts}), \tag{21}$$

$$\frac{\mathrm{d}\sigma_{13}^{e^+e^-\to e^+e^-+n\gamma}}{\mathrm{d}\Omega_1} = \int\limits_{\Delta}^{1}\int\limits_{\Delta}^{1}\int\limits_{0}^{\Delta}\int\limits_{\Delta}^{1}\mathrm{d}x_1\mathrm{d}x_2\mathrm{d}x_3\mathrm{d}x_4\mathcal{D}(z_1,s)\mathcal{D}(z_2,s)\mathcal{D}(z_3,\tilde{s})\mathcal{D}(z_4,\tilde{s}) \times\frac{\mathrm{d}\tilde{\sigma}_0(z_1,z_2)}{\mathrm{d}\Omega_1}\left(1+\frac{\alpha}{\pi}\tilde{K}_{SV}\right)\Theta(\text{cuts}), \tag{22}$$

$$\frac{\mathrm{d}\sigma_{14}^{e^+e^-\to e^+e^-+n\gamma}}{\mathrm{d}\Omega_1} = \int\limits_{\Delta}^{1}\int\limits_{0}^{\Delta}\int\limits_{\Delta}^{1}\int\limits_{\Delta}^{1}\mathrm{d}x_1\mathrm{d}x_2\mathrm{d}x_3\mathrm{d}x_4\mathcal{D}(z_1,s)\mathcal{D}(z_2,s)\mathcal{D}(z_3,\tilde{s})\mathcal{D}(z_4,\tilde{s}) \times\frac{\mathrm{d}\tilde{\sigma}_0(z_1,z_2)}{\mathrm{d}\Omega_1}\left(1+\frac{\alpha}{\pi}\tilde{K}_{SV}\right)\Theta(\text{cuts}), \tag{23}$$

$$\frac{\mathrm{d}\sigma_{15}^{e^+e^-\to e^+e^-+n\gamma}}{\mathrm{d}\Omega_1} = \int\limits_{0}^{\Delta}\int\limits_{\Delta}^{1}\int\limits_{\Delta}^{1}\int\limits_{\Delta}^{1}\mathrm{d}x_1\mathrm{d}x_2\mathrm{d}x_3\mathrm{d}x_4\mathcal{D}(z_1,s)\mathcal{D}(z_2,s)\mathcal{D}(z_3,\tilde{s})\mathcal{D}(z_4,\tilde{s}) \times\frac{\mathrm{d}\tilde{\sigma}_0(z_1,z_2)}{\mathrm{d}\Omega_1}\left(1+\frac{\alpha}{\pi}\tilde{K}_{SV}\right)\Theta(\text{cuts}). \tag{24}$$

The cross section with the emission of four jets along the momenta of each initial and final particles is written below,

$$\frac{\mathrm{d}\sigma_{16}^{e^+e^-\to e^+e^-+n\gamma}}{\mathrm{d}\Omega_1} = \int\limits_{\Delta}^{1}\int\limits_{\Delta}^{1}\int\limits_{\Delta}^{1}\int\limits_{\Delta}^{1}\mathrm{d}x_1\mathrm{d}x_2\mathrm{d}x_3\mathrm{d}x_4\mathcal{D}(z_1,s)\mathcal{D}(z_2,s)\mathcal{D}(z_3,\tilde{s})\mathcal{D}(z_4,\tilde{s}) \times\frac{\mathrm{d}\tilde{\sigma}_0(z_1,z_2)}{\mathrm{d}\Omega_1}\left(1+\frac{\alpha}{\pi}\tilde{K}_{SV}\right)\Theta(\text{cuts}). \tag{25}$$

The cross section with one hard photon emission outside the collinear region reads

$$\frac{\mathrm{d}\sigma_{17}^{e^+e^-\to e^+e^-+\gamma}}{\mathrm{d}\Omega_1} = \frac{\alpha^3}{2\pi^2 s}\int\limits_{\substack{k^0>\Delta\varepsilon\\ \theta_\gamma>\theta_0}} \frac{(WT)_\Pi}{4}\frac{\mathrm{d}\Gamma}{\mathrm{d}\Omega_1}\Theta(\text{cuts}), \tag{26}$$

where the phase-space volume can be represented as

$$\frac{\mathrm{d}\Gamma}{\mathrm{d}\Omega_1} = \frac{s x_1 x \mathrm{d}x \mathrm{d}\Omega_\gamma}{8(1 - x\sin^2\psi/2)}, \tag{27}$$

where ψ is the angle between momenta directions of the photon and final electron. The energy-momentum conservation laws allow to find the final particle energies and positron polar angle θ_2 if we assume that the electron and photon directions are known with photon energy:

$$\varepsilon_1 = \varepsilon\frac{1-x}{1-x\sin^2\psi/2}; \qquad \varepsilon_2 = \varepsilon\frac{\cos^2\psi/2 + (1-x)^2\sin^2\psi/2}{1-x\sin^2\psi/2},$$
$$\theta_2 = \arccos\left(-\frac{\varepsilon_1 c_1 + \omega\cos\theta_\gamma}{\varepsilon_2}\right). \tag{28}$$

A particular value of $\Delta\varepsilon$ has to be chosen for the simulation. The soft photon approximation requires $\Delta\varepsilon$ to be small. But a very small value of $\Delta\varepsilon$ could even produce unphysical negative cross sections for those terms in the *master* formula which are merged with *compensators*. The particular value of $\Delta\varepsilon$ chosen to perform the MC generation should therefore arise from a compromise between these two requirements. As a result, the cutoff energy $\Delta\varepsilon$ was chosen at ten electron masses to optimize the events simulation efficiency ($\Delta\varepsilon/\varepsilon \sim 1\%$). All seventeen parts of the cross section show a logarithmic $\Delta\varepsilon$-dependence, whereas their sum does not depend on $\Delta\varepsilon$ as it will be demonstrated below.

The calculation of cross section is performed by Monte-Carlo method. Since the *master* formula depends very strongly on the some variables and to increase the simulation efficiency the main singularities have been isolated. Namely: photon energy and emission angle were generated according to functions $1/\omega(\varepsilon-\omega)$ and $1/(1-\beta_e^2\cos^2\theta_\gamma)$, respectively. The main contribution to the Bhabha cross section comes from the t-channel and it was generated by the function $1/(1-\cos\theta_1)^2$.

The following selection criteria are applied to the events kinematic to calculate the cross section (the same as for CMD-2 collinear events):

- $|\Delta\theta| < 0.25$ rad, where $\Delta\theta = \theta_1 + \theta_2 - \pi$,
- $|\Delta\phi| < 0.15$ rad, where $\Delta\phi = |\phi_1 - \phi_2| - \pi$,
- $1.1 < \theta_{\rm aver} < \pi - 1.1$, where $\theta_{\rm aver} = (\theta_1 - \theta_2 + \pi)/2$,
- $p^{\perp}_{1,2} > 90$ MeV/c.

The body of the MCGPJ program consists of the two main cycles. At the first cycle the majorants are defined, at the second cycle the cross sections with the experimental selection criteria are determined. MCGPJ generator simulates an event according to weights for each cross section and fills the proper histograms, which can be compared with the experimental distributions.

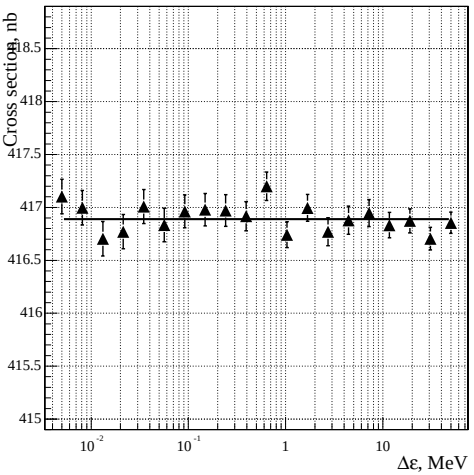

Figure 1: The dependence of cross section on the auxiliary parameter $\Delta\varepsilon$.

The numerous tests have been performed for the c.m.s. energy of 900 MeV. The cross section dependence on the auxiliary parameter $\Delta\varepsilon$ is shown in Fig. 1 after integration over the remaining kinematic variables. It is seen that cross section variations are inside the claimed precision while $\Delta\varepsilon$ changes by a factor of 10^4. The cross section variations with an auxiliary parameter θ_0 do not exceed $\pm 0.1\%$ level as it is seen in Fig. 2.

The contributions of different parts with the similar kinematics are summed and their weights in the total cross section are presented below:

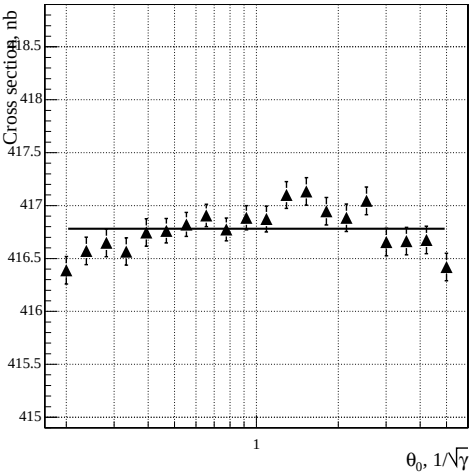

Figure 2: The dependence of cross section on the auxiliary parameter θ_0.

- $\Delta\sigma_1 \sim 55\%$: the Born cross section with virtual and soft radiative corrections;
- $\Delta\sigma_2 + \Delta\sigma_3 + \Delta\sigma_4 + \Delta\sigma_5 \sim 30\%$: relative contribution with one photon jet;
- $\Delta\sigma_6 + \Delta\sigma_7 + \Delta\sigma_8 + \Delta\sigma_9 + \Delta\sigma_{10} + \Delta\sigma_{11} \sim 3\%$: with two jets;
- $\Delta\sigma_{12} + \Delta\sigma_{13} + \Delta\sigma_{14} + \Delta\sigma_{15} \sim 0.3\%$: with three jets;
- $\Delta\sigma_{16} \sim 0.03\%$: with four jets;
- $\Delta\sigma_{17} \sim 10\%$: relative contribution with one hard photon emitted at large angles.

Comparison of the different kinematic distributions simulated by MCGPJ generator and BHWIDE [12] was performed. BHWIDE generator is based on formulae with RC the accuracy of which is about $\sim 0.5\%$. The event distributions with the parameters $\theta_1 + \theta_2 - \pi$ and $|\phi_1 - \phi_2| - \pi$ are plotted in Figs. 3, 4. Good agreement between both distributions can be seen while $\Delta\theta$ and $\Delta\phi$ vary in wide limits.

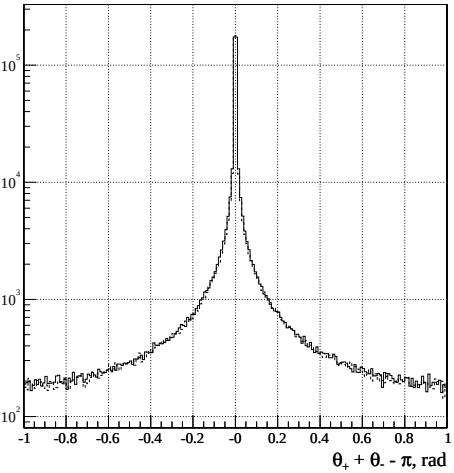

Figure 3: The events distribution with acollinearity polar angle. The solid line – MCGPJ, the dashed line – BHWIDE.

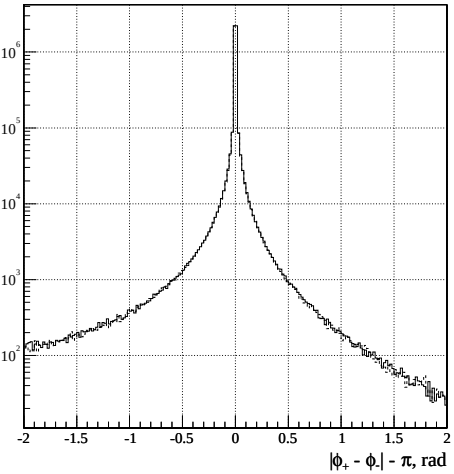

Figure 4: The events distribution with acollinearity azimuthal angle. The solid line – MCGPJ, the dashed line – BHWIDE.

The event distributions produced by both generators are presented in Fig. 5 as a function of missing energy. As one can see the spectrum shape for both distributions is close to each other except for the cutoff energy where soft and hard photons are merged. A sizable bump is observed in this point. The reason of origin this bump is slightly different dependence on the cutoff energy of the *compensators* and of the cross section with one hard photon. This fact produce a bump, but its contribution to the total cross section is negligible for our selection criteria.

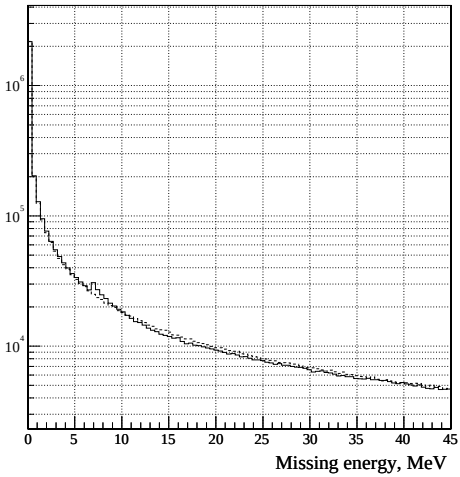

Figure 5: The events distribution with the total energy radiated by electrons and positrons. The solid line – MCGPJ, the dashed line – BHWIDE.

The relative difference of the cross sections calculated by MCGPJ code and BHWIDE with the default selection criteria is shown in Fig. 6. For the VEPP-2M energy range the difference is less than 0.1%. The visible systematic difference at 0.1% level near ρ-meson energy range is explained by the different vacuum polarization parameterization used in MCGPJ code and in BHWIDE.

The relative cross sections difference *versus* acollinearity angle is plotted in Fig. 7. As one can see, the size and sign of the difference depend on the particular choice of the angle $\Delta\theta$. The difference about of 0.5% for the angles $|\Delta\theta| \sim 0.05$ rad arises from the fact that photons inside jets should have an angular distribution, while in our code they are treated being exactly collinear to the given charged particle. The difference of about 0.3% for the large angles $|\Delta\theta| \sim 1$ rad due to the fact that BHWIDE code simulates one hard photon

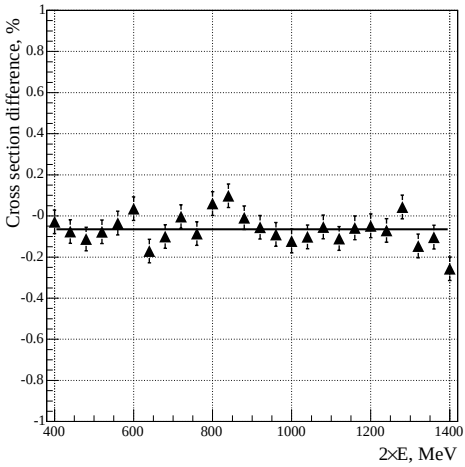

Figure 6: The relative cross sections difference calculated by MCGPJ code and BHWIDE as a function of the c.m.s. energy.

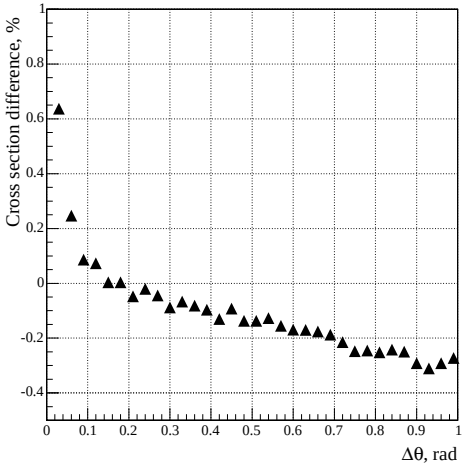

Figure 7: The relative difference between cross sections calculated by MCGPJ code and BHWIDE *versus* the acollinearity angle $|\Delta\theta|$.

only. It is worth noting that for the *soft* selection criteria MCGPJ code more correctly describes the *tails* shape of the different kinematic distributions. So, we can conclude the MCGPJ code is preferable when the soft cuts are imposed to calculate the cross section.

The crucial point to be considered is the estimate of the theoretical accuracy of this approach. In order to quantify a theoretical error, the independent comparison has been performed with the generator based on Ref. [10], where the first order corrections in α are treated exactly. It was found that the relative difference of cross sections is more than 1% for small acollinearity angles $\Delta\theta < 0.1$ rad (Fig. 8) and it is less than $\sim 0.2\%$ for acollinearity angles ~ 0.25 rad. From that it immediately follows that the radiation of two and more photons (jets) in the collinear region contributes to the cross section by amount $\sim 0.2\%$ only. Therefore we can conclude that the theoretical accuracy of the cross section with RC certainly is better than $\sim 0.2\%$ for the selection criteria mentioned above.

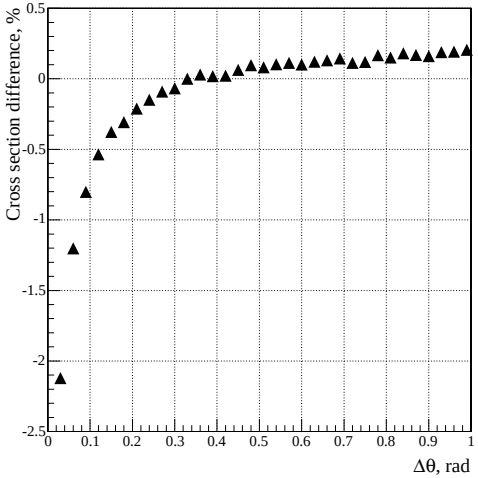

Figure 8: The relative difference between cross sections calculated by MCGPJ code and the generator based on Ref. [10] *versus* the acollinearity angle $|\Delta\theta|$.

The EM-calorimeter of the CMD-2 detector allows to separate Bhabha scattering events with a high confidence level. The dependence of the event distributions on the acollinearity angles $\Delta\theta$ and $\Delta\phi$ is presented in Figs. 9, 10. To increase the experimental statistics all data with energies greater than 1040 MeV are collected on these plots. The number of simulated events exceeds the number of the experimental events by two orders of magnitude. The momentum and angular resolutions, interaction with the detector material were added to the events kinematic parameters. The histograms were fitted by two Gaussian functions. Their relative weights and widths were the free parameters of the fit. Good agreement between experiment and simulation is clearly seen in a large scale.

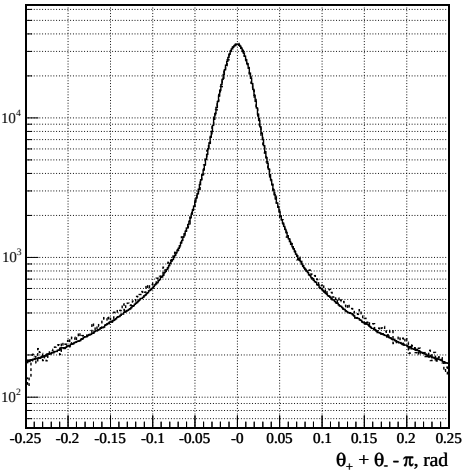

Figure 9: The event distributions *versus* acollinearity angle $\Delta\theta$ in the scattering plane. Solid line - simulation, histogram - experiment. All data with energy above 1040 MeV are collected on this plot.

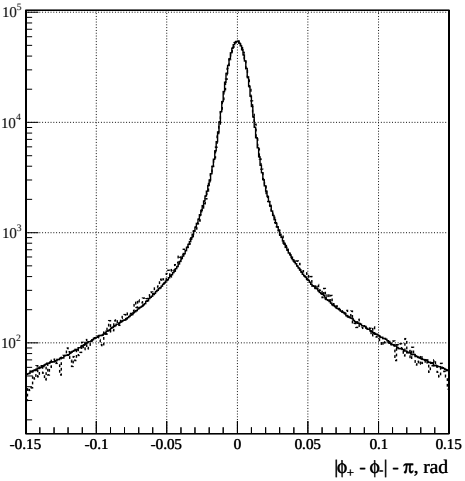

Figure 10: The event distributions *versus* acollinearity angle $\Delta\phi$ in the azimuthal plane. Solid line - simulation, histogram - experiment. All data with energy above 1040 MeV are collected on this plot.

The agreement between experiment and simulation becomes significantly worse when the MC generator based on paper [10] with $\mathcal{O}(\alpha)$ corrections is used. It can be seen in Fig. 11, Fig. 12 where two dimensional plots are presented. The points on these plots correspond to the electron and positron energies. Different population of events is observed far aside from the area where *semi-elastic* events are concentrated. About $\sim 1\%$ events have correlated low energies and they are distributed predominantly along the corridor which streches from right upper angle to the left bottom angle of this plot. The appearance of these events due to simultaneous radiation of two jets with close energies along or initial or final particles. The condition, $p^{\perp}_{1,2} > 90$ MeV/c, is very soft and only owing to this fact the integrated cross

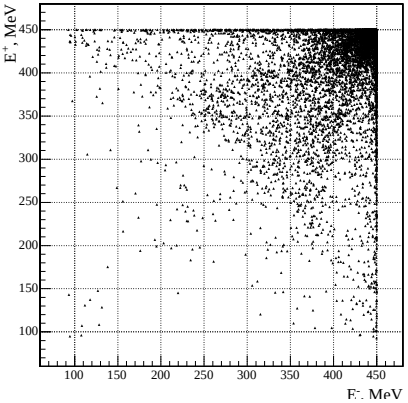

Figure 11: Two dimensional plot of the simulated events (MCGPJ) is shown. The points on this plot correspond to the electron and positron energies. The condition $\Delta\theta < 0.25$ rad can be recognized by a wide border which looks like an arc. The requirement on transverse momentum, $p^{\perp} > 250$ MeV/c, cuts off about $\sim 1\%$ events.

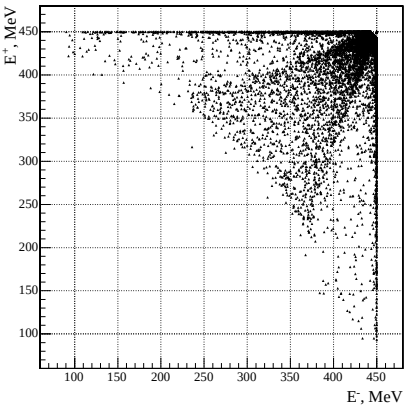

Figure 12: Two dimensional plot of the simulated events is shown. The generator is based on Ref. [10]. The points on this plot correspond to the electron and positron energies. The condition $\Delta\theta < 0.25$ rad clerarly seen by the arc of curve which divedes the field of plot on two parts (with and without events). The requirement on transverse momentum, $p^{\perp} > 250$ MeV/c, cuts off about $\sim 0.2\%$ events.

sections are equal to each other within $\sim 0.2\%$. If this condition changes to the value, $p^{\perp}_{1,2} > 250$ MeV/c, the relative difference increases up to $\sim 1\%$ as it is seen in Fig. 13, where this difference is presented as a function of the transverse momentum $p^{\perp}_{1,2}$. For the large value $p^{\perp}_{1,2} > 350$ MeV/c the difference changes a sign and quickly grows up. The cross section with photon jets becomes smaller than with one photon. This feature has a simple explanation. The distribution width of the *semi-elastic* events on the first plot is broader than for the second one due to many soft photons radiation and, as a result, these events are *smeared* more broadly near the peak area.

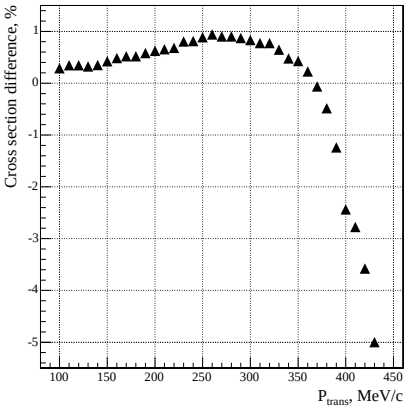

Figure 13: The difference between cross sections calculated with MCGPJ code and Ref. [10] as a function of the cut imposed on the transverse momenta of the final particles.

At the end of this section it is worth to stress that the QED radiative corrections, coming from collinear region and proportional to $(\alpha/\pi)\ln(s/m_e^2)$, are included by means of Structure Function formalism in several orders of α[1]. The exact $\mathcal{O}(\alpha)$ matrix element describing hard photon emission beyond the collinear region is implemented in the *master* formula together with *compensators*. One loop virtual corrections and due to soft photons emission are treated in the first order of α exactly. The vacuum polarization effects are inserted into photon propagators for all amplitudes describing this process. The theoretical accuracy of this approach is estimated to be 0.2% for the soft selection criteria.

[1]We can get a complete result for leading logarithmic RC up to the fifth order in α plus exponentiation of a certain part of terms.

3 Monte-Carlo generator for production of muon pairs

The same approach was used to build the MC generator to simulate muon pairs production in the reaction,

$$e^-(z_1 p_-) + e^+(z_2 p_+) \to \mu^-(p_1) + \mu^+(p_2),$$

when the initial particles lose some energy by photon jets emission in the collinear region. The *shifted* Born cross section $\mathrm{d}\tilde{\sigma}(z_1, z_2)$, modified by vacuum polarization effects in the photon propagator, according to Ref. [6] has the form

$$\frac{\mathrm{d}\tilde{\sigma}_0^{e^+e^-\to\mu^+\mu^-}(z_1,z_2)}{\mathrm{d}\Omega_1} = \frac{\alpha^2}{4s}\frac{1}{\mid 1-\Pi(z_1 z_2 s)\mid^2} \times \frac{y_1\left[z_1^2(Y_1-y_1c_1)^2 + z_2^2(Y_1+y_1c_1)^2 + 8z_1z_2m_\mu^2/s\right]}{z_1^3 z_2^3\left[z_1+z_2-(z_1-z_2)c_1Y_1/y_1\right]}, \qquad (29)$$

where $y_{1,2}^2 = Y_{1,2}^2 - 4m_\mu^2/s$; $x_{1,2} = \omega_{1,2}/\varepsilon$ are the relative energies of photon jets; $z_{1,2} = 1 - x_{1,2}$ are the relative energies of electron and positron; $Y_{1,2} = \varepsilon_{1,2}/\varepsilon$ are the relative energies of muons; $c_1 = \cos\theta_1$, θ_1 is the polar angle of negative muon with respect to the electron beam direction. The energy-momentum conservation laws,

$$z_1 + z_2 = Y_1 + Y_2, \quad z_1 - z_2 = y_1c_1 + y_2c_2, \quad y_1\sqrt{1-c_1^2} = y_2\sqrt{1-c_2^2},$$

allow to determine Y_1, Y_2 and positron polar angle θ_2 ($c_2 = \cos\theta_2$):

$$\begin{aligned} Y_1 &= \frac{2m_\mu^2}{s}\frac{(z_2-z_1)c_1}{z_1z_2 + [z_1^2z_2^2 - (m_\mu^2/s)((z_1+z_2)^2 - (z_1-z_2)^2c_1^2)]^{1/2}} \\ &\quad + \frac{2z_1z_2}{z_1+z_2-c_1(z_1-z_2)}, \qquad c_2 = \frac{z_1-z_2-y_1c_1}{y_2} \end{aligned} \qquad (30)$$

The charge-even part of the cross section in the first order of α arises as one-loop virtual and soft radiative corrections and according to Ref. [6] it is convenient to present in the next form:

$$\begin{aligned} \frac{\mathrm{d}\sigma_{even}^{S+V}}{\mathrm{d}\Omega_1} &= \frac{\mathrm{d}\tilde{\sigma}_0^{e^+e^-\to\mu^+\mu^-}(1,1)}{\mathrm{d}\Omega_1}\frac{2\alpha}{\pi}(A_e + A_\mu), \\ A_e &= (L-1)\ln\frac{\Delta\varepsilon}{\varepsilon} + \frac{3}{4}(L-1) + \frac{\pi^2}{6} - \frac{1}{4}, \\ A_\mu &= \left(\frac{1+\beta^2}{2\beta}\ln\frac{1+\beta}{1-\beta} - 1\right)\ln\frac{\Delta\varepsilon}{\varepsilon} + K_{\mathrm{even}}^{\mu}. \end{aligned} \qquad (31)$$

The expression for the value $K^{\mu}_{\rm even}$ was derived in papers [13, 6] and it reads

$$
\begin{aligned}
K^{\mu}_{\rm even} &= -1+\rho\left(\frac{1+\beta^2}{2\beta}-\frac{1}{2}+\frac{1}{4\beta}\right)+\ln\frac{1+\beta}{2}\left(\frac{1}{2\beta}+\frac{1+\beta^2}{\beta}\right) \qquad (32)\\
&- \frac{1-\beta^2}{2\beta}\frac{l_\beta}{2-\beta^2(1-c_1^2)}+\frac{1+\beta^2}{2\beta}\left[\frac{\pi^2}{6}+2{\rm Li}_2\left(\frac{1-\beta}{1+\beta}\right)+l_\beta\ln\frac{1+\beta}{2\beta^2}\right],\\
l_\beta &= \ln\frac{1+\beta}{1-\beta}, \quad \rho=\ln\frac{s}{m_\mu^2}, \quad L=\ln\frac{s}{m_e^2}, \quad {\rm Li}_2(x)\equiv-\int\limits_0^x\frac{{\rm d}t}{t}\ln(1-t).
\end{aligned}
$$

The charge-odd part of the cross section comes from the interference of the Born amplitude and box-type diagrams and with amplitudes describing soft photon emission by the initial and final particles [13]. According to Ref. [6] the corresponding expression is given by

$$
\frac{{\rm d}\sigma^{S+V}_{\rm odd}}{{\rm d}\Omega_1}=\frac{{\rm d}\sigma_0^{e^+e^-\to\mu^+\mu^-}(1,1)}{{\rm d}\Omega_1}\frac{2\alpha}{\pi}\left(2\ln\frac{\Delta\varepsilon}{\varepsilon}\ln\frac{1-\beta c_1}{1+\beta c_1}+K^{\mu}_{\rm odd}\right), \qquad (33)
$$

where

$$
\begin{aligned}
K^{\mu}_{\rm odd} &= \frac{1}{2}l_-^2-L_-(\rho+l_-)+{\rm Li}_2\left(\frac{1-\beta^2}{2(1-\beta c_1)}\right)+{\rm Li}_2\left(\frac{\beta^2(1-c_1^2)}{1+\beta^2-2\beta c_1}\right)\\
&- \int\limits_0^{1-\beta^2}\frac{{\rm d}x}{x}f(x)\left(1-\frac{x(1+\beta^2-2\beta c_1)}{(1-\beta c_1)^2}\right)^{-\frac{1}{2}}+\frac{1}{2-\beta^2(1-c_1^2)}\\
&\times\left\{-\frac{1-2\beta^2+\beta^2c_1^2}{1+\beta^2-2\beta c_1}(\rho+l_-)-\frac{1}{4}(1-\beta^2)\left[l_-^2-2L_-(l_-+\rho)\right.\right.\\
&\left.+2{\rm Li}_2\left(\frac{1-\beta^2}{2(1-\beta c_1)}\right)\right]+\beta c_1\left[-\frac{\rho}{2\beta^2}+\left(\frac{\pi^2}{12}+\frac{1}{4}\rho^2\right)\left(1-\frac{1}{\beta}-\frac{\beta}{2}+\frac{1}{2\beta^3}\right)\right.\\
&+\frac{1}{\beta}(-1-\frac{\beta^2}{2}+\frac{1}{2\beta^2})\left(\rho\ln\frac{1+\beta}{2}-2{\rm Li}_2\left(\frac{1-\beta}{2}\right)-{\rm Li}_2\left(-\frac{1-\beta}{1+\beta}\right)\right)\\
&\left.\left.-\frac{1}{2}l_-^2+L_-(\rho+l_-)-{\rm Li}_2\left(\frac{1-\beta^2}{2(1-\beta c_1)}\right)\right]\right\}-(c_1\to-c_1), \qquad (34)\\
f(x) &= \left(\frac{1}{\sqrt{1-x}}-1\right)\ln\frac{\sqrt{x}}{2}-\frac{1}{\sqrt{1-x}}\ln\frac{1+\sqrt{1-x}}{2},\\
l_- &= \ln\frac{1-\beta c_1}{2}, \qquad L_-=\ln\left(1-\frac{1-\beta^2}{2(1-\beta c_1)}\right).
\end{aligned}
$$

The muons cross section production with one hard photon emission was studied in detail elsewhere [14, 15, 6]. This cross section in the differential form, keeping the relevant information about the kinematics of the final particles, can be written according to [6]:

$$\begin{aligned} \mathrm{d}\sigma^{e^+e^-\to\mu^+\mu^-\gamma}_{\rm hard} &= \frac{\alpha^3}{2\pi^2 s^2} R^{e^+e^-\to\mu^+\mu^-\gamma}_{\rm hard}\mathrm{d}\Gamma, \\ \mathrm{d}\Gamma &= \frac{d^3p_1}{\varepsilon_1}\frac{d^3p_2}{\varepsilon_2}\frac{d^3k}{\omega}\delta^{(4)}(p_- + p_+ - p_1 - p_2 - k) \\ &= \frac{s\beta_1 \mathrm{d}\Omega_1 x \mathrm{d}x \mathrm{d}\Omega_\gamma}{4(2 - x(1 - \cos\psi/\beta_1))}, \end{aligned} \tag{35}$$

where $\mathrm{d}\Gamma$ is a phase-space volume of the three particles in the final state, β_1 is a velocity of negative muon, δ-function provides the energy-momentum conservation.

The quantity $R^{e^+e^-\to\mu^+\mu^-\gamma}_{\rm hard}$ consists of three terms and describes one hard photon emission outside the narrow cones. It includes photon emission by the initial and final particles as well as their interference:

$$R^{e^+e^-\to\mu^+\mu^-\gamma}_{\rm hard} = \frac{s}{16(4\pi\alpha)^3}\sum_{spins}|M|^2 = R_{ee} + R_{e\mu} + R_{\mu\mu}, \tag{36}$$

$$\begin{aligned} R_{ee} &= \frac{1}{|1-\Pi(s_1)|^2}\left[C\frac{s}{\chi_-\chi_+} + \frac{m_\mu^2}{s_1^2}\Delta_{s_1 s_1}\right. \\ &\left. -\frac{m_e^2}{2\chi_-^2}\frac{(t_1^2+u_1^2+2m_\mu^2 s_1)}{s_1^2} - \frac{m_e^2}{2\chi_+^2}\frac{(t^2+u^2+2m_\mu^2 s_1)}{s_1^2}\right], \\ R_{e\mu} &= \Re\mathrm{e}\frac{1}{(1-\Pi(s_1))(1-\Pi(s))^*} \\ &\times\left[C\left(\frac{u}{\chi_-\chi'_+} + \frac{u_1}{\chi_+\chi'_-} - \frac{t}{\chi_-\chi'_-} - \frac{t_1}{\chi_+\chi'_+}\right) + \frac{m_\mu^2}{ss_1}\Delta_{ss_1}\right] \\ R_{\mu\mu} &= \frac{1}{|1-\Pi(s)|^2}\left[\frac{s_1}{\chi'_-\chi'_+}C + \frac{m_\mu^2}{s^2}\Delta_{ss}\right], \quad C = \frac{u^2+u_1^2+t^2+t_1^2}{4ss_1}, \end{aligned}$$

$$
\begin{aligned}
\Delta_{s_1 s_1} &= \frac{(t+u)^2+(t_1+u_1)^2}{2\chi_-\chi_+}, \\
\Delta_{ss} &= -\frac{u^2+t_1^2+2sm_\mu^2}{2(\chi'_-)^2} - \frac{u_1^2+t^2+2sm_\mu^2}{2(\chi'_+)^2} + \\
&\quad + \frac{1}{\chi'_-\chi'_+}\big(ss_1 - s^2 + tu + t_1u_1 - 2sm_\mu^2\big), \\
\Delta_{ss_1} &= \frac{s+s_1}{2}\left(\frac{u}{\chi_-\chi'_+} + \frac{u_1}{\chi_+\chi'_-} - \frac{t}{\chi_-\chi'_-} - \frac{t_1}{\chi_+\chi'_+}\right) \\
&\quad + \frac{2(u-t_1)}{\chi'_-} + \frac{2(u_1-t)}{\chi'_+}.
\end{aligned}
$$

Mandelstam variables and new introduced quantities in these notations are defined as:

$$
s = 2p_+p_-, \quad s_1 = (p_1+p_2)^2, \quad t = -2p_-p_1, \quad t_1 = -2p_+p_2,
$$

$$
u = -2p_-p_2, \quad u_1 = -2p_+p_1, \quad \chi_\pm = p_\pm k, \quad \chi'_\pm = p_{1,2}k.
$$

As well as for Bhabha scattering events the main contribution to the cross section is connected with photons emission in the collinear region [11, 6]. The muon's cross section integrated inside narrow cones around motion of the initial particles is presented by two terms:

$$
\mathrm{d}\sigma_{\mathrm{coll}}^{e^+e^-\to\mu^+\mu^-\gamma} = \frac{\alpha}{\pi}(L-1)\int\limits_\Delta^1 \mathrm{d}x \frac{1+(1-x)^2}{x}\Big[\mathrm{d}\tilde{\sigma}_0(1-x,1) + \mathrm{d}\tilde{\sigma}_0(1,1-x)\Big]
$$

$$
+\frac{\alpha}{\pi}\int\limits_\Delta^1 \mathrm{d}x\left(x + \frac{1+(1-x)^2}{x}\ln\frac{\theta_0^2}{4}\right)\Big[\mathrm{d}\tilde{\sigma}_0(1-x,1) + \mathrm{d}\tilde{\sigma}_0(1,1-x)\Big]. \qquad (37)
$$

The first term in this expression, proportional to $(\alpha/\pi)(L-1)$, is taken into account in $\mathcal{D}$-functions. The remaining term is a so-called *compensator*. These two *compensators* provide the cross section independence in Eq. (38) with an auxiliary parameter θ_0. Similar to Bhabha cross section the construction of the *master* formula describing the process of muon pairs production reads

$$\frac{\mathrm{d}\sigma^{e^+e^-\to\mu^+\mu^-+n\gamma}}{\mathrm{d}\Omega_1} =$$

$$= \int\limits_0^1\int\limits_0^1 \mathrm{d}x_1\mathrm{d}x_2\mathcal{D}(z_1,s)\mathcal{D}(z_2,s)\frac{\mathrm{d}\tilde{\sigma}_0(z_1,z_2)}{\mathrm{d}\Omega_1}\big(1+\frac{2\alpha}{\pi}\tilde{K}\big)\Theta(\mathrm{cuts})$$

$$+\frac{\alpha}{\pi}\int\limits_\Delta^1 \frac{\mathrm{d}x_1}{x_1}\left[\big(z_1+\frac{x_1^2}{2}\big)\ln\frac{\theta_0^2}{4}+\frac{x_1^2}{2}\right]\frac{\mathrm{d}\tilde{\sigma}_0(z_1,1)}{\mathrm{d}\Omega_1}\Theta(\mathrm{cuts})$$

$$+\frac{\alpha}{\pi}\int\limits_\Delta^1 \frac{\mathrm{d}x_2}{x_2}\left[\big(z_2+\frac{x_2^2}{2}\big)\ln\frac{\theta_0^2}{4}+\frac{x_2^2}{2}\right]\frac{\mathrm{d}\tilde{\sigma}_0(1,z_2)}{\mathrm{d}\Omega_1}\Theta(\mathrm{cuts})$$

$$+\frac{\alpha^3}{2\pi^2 s^2}\int\limits_{\substack{k^0>\Delta\varepsilon\\ \theta_\gamma>\theta_0}} R^{e^+e^-\to\mu^+\mu^-\gamma}_{\mathrm{hard}}\frac{\mathrm{d}\Gamma}{\mathrm{d}\Omega_1}\Theta(\mathrm{cuts})$$

$$+\frac{2\alpha}{\pi}\left[\frac{1+\beta^2}{2\beta}\ln\frac{1+\beta}{1-\beta}-1+2\ln\frac{1-\beta c_1}{1+\beta c_1}\right]\ln(\frac{\Delta\varepsilon}{\varepsilon})\cdot\frac{\mathrm{d}\tilde{\sigma}_0(1,1)}{\mathrm{d}\Omega_1}, \quad (38)$$

where $\tilde{K}=\pi^2/6-1/4+K^\mu_{\mathrm{even}}(\tilde{s},\tilde{\theta_1})+K^\mu_{\mathrm{odd}}(\tilde{s},\tilde{\theta_1})$; $\tilde{\theta_1}$ is a negative muon polar angle in center-of-mass system,

$$\tilde{c_1}=\sqrt{\frac{z_1z_2-Y_1^2(1-c_1^2)-c_1^2(1-\beta^2)}{z_1z_2-(1-\beta^2)}};$$

$\Theta(\mathrm{cuts})$ is a step-function equal to 1 or 0 if kinematic variables meet the demands or not to selection criteria; condition, $\theta_\gamma > \theta_0$, means that the photon angle must be outside of the narrow cones with respect to the beam axis.

Let us enumerate some essential improvements which are contained in the *master* formula and which provide the cross section accuracy $\sim 0.2\%$:

- the cross section contains the enhanced contributions with photon jets emission in the collinear region together with two *compensators*;
- two *compensators* are incorporated into *master* formula to exclude the cross section dependence with the auxiliary parameter θ_0;
- the cross section with one-loop virtual and soft corrections are taken into account exactly;

- the cross section with one hard photon emission outside the narrow cones [6] contains all terms proportional to m_μ^2/s;
- the vacuum polarization effects are inserted into photon propagators for the all Feynman diagrams.

In order to build MC generator, simulating the process $e^+e^- \to \mu^+\mu^-(n\gamma)$, the integration limits of the first term in Eq. (38) were divided into two parts from 0 to $\Delta\varepsilon$ and from $\Delta\varepsilon$ to the maximal jet energy. As a result, two-fold integral splits into four separate contributions. Those of them describing one photon jet radiation are combined in a proper way with *compensators* in the *master* formula as it was done for the events of Bhabha scattering. The total cross section does not depend on the auxiliary parameters $\Delta\varepsilon$ and θ_0.

The first contribution includes the effects due to soft and virtual radiative corrections and it is:

$$\frac{\mathrm{d}\sigma_1^{e^+e^-\to\mu^+\mu^-(n\gamma)}}{\mathrm{d}\Omega_1} = \int\limits_0^\Delta\int\limits_0^\Delta \mathrm{d}x_1\mathrm{d}x_2\mathcal{D}(z_1,s)\mathcal{D}(z_2,s)\big(1+\frac{2\alpha}{\pi}\tilde{K}\big)\frac{\mathrm{d}\tilde{\sigma}_0(z_1,z_2)}{\mathrm{d}\Omega_1}$$
$$+\frac{2\alpha}{\pi}\left[\frac{1+\beta^2}{2\beta}\ln\frac{1+\beta}{1-\beta}-1+2\ln\frac{1-\beta c_1}{1+\beta c_1}\right]\ln\frac{\Delta\varepsilon}{\varepsilon}\frac{\mathrm{d}\tilde{\sigma}_0(1,1)}{\mathrm{d}\Omega_1}\,. \qquad (39)$$

The contribution of a single jet emission along the electron beam is given by

$$\frac{\mathrm{d}\sigma_2^{e^+e^-\to\mu^+\mu^-+n\gamma}}{\mathrm{d}\Omega_1} = \int\limits_\Delta^1\int\limits_0^\Delta \mathrm{d}x_1\mathrm{d}x_2\mathcal{D}(z_2,s)\left[\mathcal{D}(z_1,s)\big(1+\frac{2\alpha}{\pi}\tilde{K}\big)\right.$$
$$\left.+\frac{\alpha}{\pi}\frac{1}{x_1}\left(\big(z_1+\frac{x_1^2}{2}\big)\ln\frac{\theta_0^2}{4}+\frac{x_1^2}{2}\right)\right]\frac{\mathrm{d}\tilde{\sigma}_0(z_1,z_2)}{\mathrm{d}\Omega_1}\Theta(\text{cuts}), \qquad (40)$$

where the *compensator* is included to describe exactly the angular distribution of one hard photon inside and outside of the narrow cones.

The analogous contribution with a hard jet along the incoming positron reads

$$\frac{\mathrm{d}\sigma_3^{e^+e^-\to\mu^+\mu^-+n\gamma}}{\mathrm{d}\Omega_1} = \int\limits_0^\Delta\int\limits_\Delta^1 \mathrm{d}x_1\mathrm{d}x_2\mathcal{D}(z_1,s)\left[\mathcal{D}(z_2,s)\big(1+\frac{2\alpha}{\pi}\tilde{K}\big)\right.$$
$$\left.+\frac{\alpha}{\pi}\frac{1}{x_2}\left(\big(z_2+\frac{x_2^2}{2}\big)\ln\frac{\theta_0^2}{4}+\frac{x_2^2}{2}\right)\right]\frac{\mathrm{d}\tilde{\sigma}_0(z_1,z_2)}{\mathrm{d}\Omega_1}\Theta(\text{cuts}). \qquad (41)$$

The cross section with emission of two hard jets along motion of the both initial particles is presented below,

$$\frac{\mathrm{d}\sigma_4^{e^+e^-\to\mu^+\mu^-+n\gamma}}{\mathrm{d}\Omega_1} =$$

$$= \int\limits_{\Delta}^{1}\int\limits_{\Delta}^{1} \mathrm{d}x_1\mathrm{d}x_2\mathcal{D}(z_1,s)\mathcal{D}(z_2,s)\big(1+\frac{2\alpha}{\pi}\tilde{K}\big)\frac{\mathrm{d}\tilde{\sigma}_0(z_1,z_2)}{\mathrm{d}\Omega_1}\Theta(\text{cuts}). \quad (42)$$

The last part is the cross section with one hard photon emission outside narrow cones and is given by

$$\frac{\mathrm{d}\sigma_5^{e^+e^-\to\mu^+\mu^-+\gamma}}{\mathrm{d}\Omega_1} = \frac{\alpha^3}{2\pi^2 s^2}\int\limits_{\substack{k^0>\Delta\varepsilon\\ \theta_\gamma>\theta_0}} R_{\text{hard}}^{e^+e^-\to\mu^+\mu^-\gamma}\frac{\mathrm{d}\Gamma}{\mathrm{d}\Omega_1}\Theta(\text{cuts}). \quad (43)$$

The numerical tests have been performed for the c.m.s. energy of 900 MeV. Figs. 14, 15 show the independence of the cross section with respect to the auxiliary parameters $\Delta\varepsilon$ and θ_0 in a broad range of their values. The cross section deviations do not exceed $\pm 0.1\%$ when Δ and θ_0 change their values more than four orders of magnitude.

Comparison with the KKMC [16] generator was performed. The theoretical accuracy of the formulae on which KKMC based on is about $\sim 0.1\%$. The existing code in KKMC does not provide the correct description of the vacuum polarization effects in photon propagator at low energies, so it was switched off in both generators. The cutoff energy of the soft photons was chosen to be 0.1 MeV. The relative difference between cross sections produced by MCGPJ generator and KKMC in the VEPP-2M energy range is presented in Fig. 16. Good agreement at the level of our precision $\pm 0.2\%$ is seen.

Comparison with the experimental data has been done too. The results for the double ratio are presented in Fig. 17 for the low energy range, where the CMD-2 detector resolution is enough to distinguish pions, muons and electrons. The ratio of the number of selected muons to that of electrons divided by the ratio of the theoretical cross sections, $\sigma(ee\to\mu\mu)/\sigma(ee\to ee)$, in average does not exceed 1.4 % with the statistical and systematic errors about ~ 1.4 % and ~ 0.7 %, respectively. Unfortunately a scare experimental statistics in this energy range does not allow to evaluate the comparisons with a better accuracy.

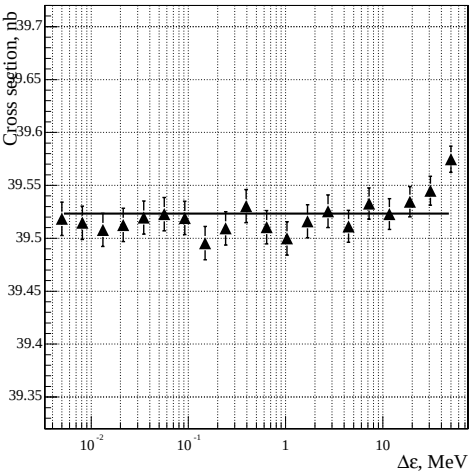

Figure 14: Dependence of the $\mu^+\mu^-$ cross section on the auxiliary parameter $\Delta\varepsilon$.

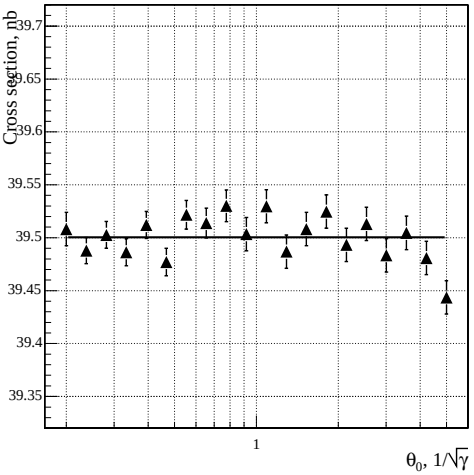

Figure 15: Dependence of the $\mu^+\mu^-$ cross section on the auxiliary parameter θ_0.

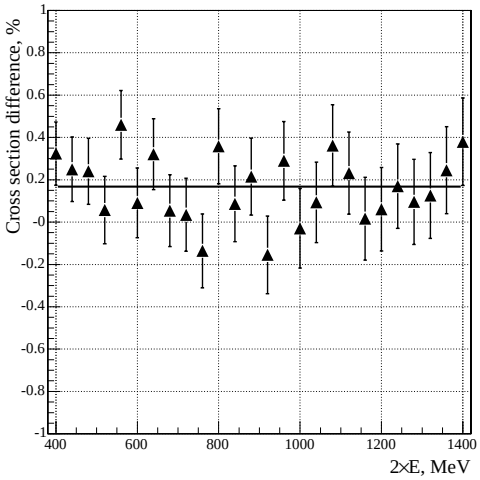

Figure 16: The relative difference between cross sections calculated by MCGPJ and KKMC *versus* the c.m.s. energy.

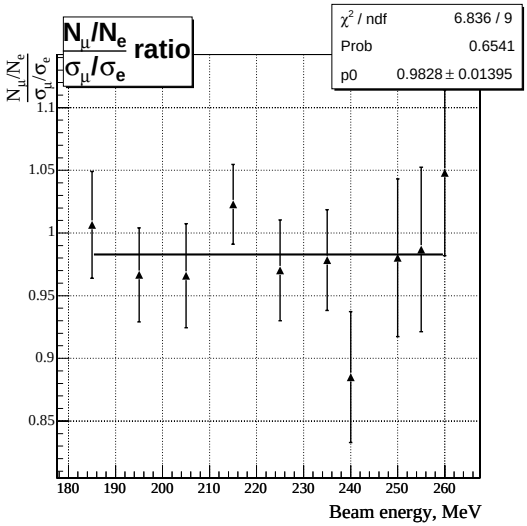

Figure 17: The ratio of the numbers of the selected muon and electron pairs divided by the ratio of the corresponding theoretical cross sections.

4 Monte-Carlo generator for production of pion pairs

The same ideas and technique were applied for the processes $e^+e^- \to \pi^+\pi^-$, K^+K^-, K_SK_L to build the MC generator with the RC considering pseudoscalar mesons as point-like objects. For the precise accounting of RC results of Refs. [7, 9] were used. As it was described before the leading contributions, which are proportional to $(\alpha/\pi)^n \ln^n(s/m_e^2)$, are taken into account by means of SF formalism. The one loop virtual corrections and those due to the emission of real soft photons as well as one hard photon emission outside the collinear region are included in the first order of α exactly.

According to the paper [7] the *shifted* Born cross section is given by the expression

$$\begin{aligned}\frac{\mathrm{d}\tilde{\sigma}_0^{e^+e^-\to\pi^+\pi^-}(z_1,z_2)}{\mathrm{d}\Omega_1} &= \frac{\alpha^2}{4s}\frac{(Y_1^2-m_\pi^2/\varepsilon^2)^{3/2}}{z_1^2z_2^2} \\ &\times \frac{(1-c_1^2)|F_\pi(sz_1z_2)|^2}{z_1+z_2+(z_2-z_1)(1-m_\pi^2/(\varepsilon^2Y_1^2))^{-1/2}c_1},\end{aligned} \tag{44}$$

where $z_{1,2}$ are the energy fractions of the electron and positron after photon jets radiation in the collinear region, $|F_\pi(sz_1z_2)|^2$ is a pion form factor squared, $c_1 = \cos\theta_1$, θ_1 is a polar angle of the negative pion momentum with respect to the direction of the electron beam. The energy fractions $Y_{1,2}$ of the final pions and a polar angle of the positive pion, θ_2, can be found from the following kinematic relations:

$$z_1+z_2 = Y_1+Y_2, \quad z_1-z_2 = y_1c_1+y_2c_2, \quad y_1\sqrt{1-c_1^2} = y_2\sqrt{1-c_2^2},$$

where $y_{1,2}^2 = Y_{1,2}^2 - 4m_\pi^2/s$. From these equations we can obtain:

$$\begin{aligned}Y_1 &= \frac{2z_1z_2}{z_1+z_2-c_1(z_1-z_2)} \\ &- \frac{2m_\pi^2}{s}\cdot\frac{(z_1-z_2)c_1}{z_1z_2+\sqrt{z_1^2z_2^2-(m_\pi^2/s)((z_1+z_2)^2-(z_1-z_2)^2c_1^2)}}, \\ Y_2 &= z_1+z_2-Y_1, \quad c_2 = -(z_1-z_2-y_1c_1)/y_2.\end{aligned} \tag{45}$$

The formulae with charge-even and charge-odd parts of the cross sections due to soft and virtual photons radiation [17, 18] were rewrited according to

paper [7]. The charge-even part is convenient to present in the following way:

$$\frac{\mathrm{d}\sigma_{\mathrm{even}}^{S+V}}{\mathrm{d}\Omega_1} = \frac{\mathrm{d}\sigma_0^{ee\to\pi\pi}(1,1)}{\mathrm{d}\Omega_1}\cdot\frac{2\alpha}{\pi}(A_e + A_\pi), \tag{46}$$

where A_e and A_π are given by [7]

$$\begin{aligned} A_e &= (L-1)\ln\frac{\Delta\varepsilon}{\varepsilon} + \frac{3}{4}(L-1) + \frac{\pi^2}{6} - \frac{1}{4}, \\ A_\pi &= \left(\frac{1+\beta^2}{2\beta}\ln\frac{1+\beta}{1-\beta} - 1\right)\ln\frac{\Delta\varepsilon}{\varepsilon} + K_{\mathrm{even}}^{\pi}. \end{aligned} \tag{47}$$

The expression for the quantity K_{even}^{π} can be found in [7, 18],

$$\begin{aligned} K_{\mathrm{even}}^{\pi} &= -1 + \frac{1-\beta}{2\beta}\rho + \frac{2+\beta^2}{\beta}\ln\frac{1+\beta}{2} \\ &+ \frac{1+\beta^2}{2\beta}\left[\rho + \frac{\pi^2}{6} + l_\beta\ln\frac{1+\beta^2}{2\beta^2} + 2\mathrm{Li}_2\frac{1-\beta}{1+\beta}\right]. \end{aligned} \tag{48}$$

The corresponding contribution to the charge-odd part is the interference result of the Born amplitudes with the amplitudes describing box-type diagrams and soft photons emission by electrons and pions [19]. According to paper [7] this expression can be presented in the following form:

$$\frac{\mathrm{d}\sigma_{\mathrm{odd}}^{S+V}}{\mathrm{d}\Omega_1} = \frac{\mathrm{d}\sigma_0^{ee\to\pi\pi}(1,1)}{\mathrm{d}\Omega_1}\cdot\frac{2\alpha}{\pi}\left(2\ln\frac{\Delta\varepsilon}{\varepsilon}\ln\frac{1-\beta c_1}{1+\beta c_1} + K_{\mathrm{odd}}^{\pi}\right), \tag{49}$$

where K_{odd}^{π}, in one's turn, is equal to

$$\begin{aligned} K_{\mathrm{odd}}^{\pi} &= \frac{1}{2}l_-^2 - \mathrm{Li}_2\left(\frac{1-2\beta c_1+\beta^2}{2(1-\beta c_1)}\right) + \mathrm{Li}_2\left(\frac{\beta^2(1-c_1^2)}{1-2\beta c_1+\beta^2}\right) \\ &- \int_0^{1-\beta^2}\frac{\mathrm{d}x}{x}f(x)\left(1 - \frac{x(1-2\beta c_1+\beta^2)}{(1-\beta c_1)^2}\right)^{-\frac{1}{2}} \\ &+ \frac{1}{2\beta^2(1-c_1^2)}\left\{\left[\frac{1}{2}l_-^2 - (L+l_-)L_- + \mathrm{Li}_2\left(\frac{1-\beta^2}{2(1-\beta c_1)}\right)\right](1-\beta^2)\right. \\ &+ (1-\beta c_1)\left[-l_-^2 - 2\mathrm{Li}_2\left(\frac{1-\beta^2}{2(1-\beta c_1)}\right) + 2(L+l_-)L_-\right. \end{aligned} \tag{50}$$

$$
\begin{aligned}
&- \frac{(1-\beta)^2}{2\beta}\left(\frac{1}{2}L^2+\frac{\pi^2}{6}\right)+\frac{1+\beta^2}{\beta}\left(L\ln\frac{2}{1+\beta}-\mathrm{Li}_2\left(-\frac{1-\beta}{1+\beta}\right)\right.\\
&\left.+\ 2\mathrm{Li}_2\left(\frac{1-\beta}{2}\right)\right)\Big]\Bigg\}-(c_1\to -c_1),\\
f(x) &= \left(\frac{1}{\sqrt{1-x}}-1\right)\ln\frac{\sqrt{x}}{2}-\frac{1}{\sqrt{1-x}}\ln\frac{1+\sqrt{1-x}}{2}, \qquad (51)\\
l_- &= \ln\frac{1-\beta c_1}{2}, \qquad L_-=\ln\left(1-\frac{1-\beta^2}{2(1-\beta c_1)}\right).
\end{aligned}
$$

The cross section of the pion pairs production with one hard photon emission in the reaction, $e^+e^-\to\pi^+\pi^-\gamma$, was studied in [17]. In the differential form preserving the complete kinematics of the final state particles, it is convenient to write it according to Ref. [7]:

$$
\begin{aligned}
\frac{\mathrm{d}\sigma^{e^+e^-\to\pi^+\pi^-\gamma}_{\mathrm{hard}}}{\mathrm{d}\Omega_1} &= \frac{\alpha^3}{32\pi^2 s}R^{e^+e^-\to\pi^+\pi^-\gamma}_{\mathrm{hard}}\frac{\mathrm{d}\Gamma}{\mathrm{d}\Omega_1},\\
\frac{\mathrm{d}\Gamma}{\mathrm{d}\Omega_1} &= \int\frac{\mathrm{d}^3p_1}{\varepsilon_1}\frac{\mathrm{d}^3p_2}{\varepsilon_2}\frac{\mathrm{d}^3k}{\omega}\delta^{(4)}(p_-+p_+-p_1-p_2-k)\\
&= \frac{s\beta_1 x\mathrm{d}x\mathrm{d}\Omega_\gamma}{4(2-x(1-\cos\psi/\beta_1))}, \qquad (52)
\end{aligned}
$$

where $\mathrm{d}\Gamma$ is a phase space of the three particles in the final state, δ-function provides the energy-momentum conservation low. Quantity $R^{e^+e^-\to\pi^+\pi^-\gamma}_{\mathrm{hard}}$ consists of three terms which describe the initial state radiation, final state radiation, and their interference:

$$
\begin{aligned}
R^{e^+e^-\to\pi^+\pi^-\gamma}_{\mathrm{hard}} &= R_{ee}+R_{\pi\pi}+R_{e\pi}, \qquad (53)\\
R_{ee} &= |F_\pi(s_1)|^2\left\{A\frac{4s}{\chi_-\chi_+}-\frac{8m_e^2}{s_1^2}\left(\frac{t_1u_1}{\chi_-^2}+\frac{tu}{\chi_+^2}\right)\right.\\
&\left.+\frac{8m_e^2m_\pi^2}{s_1}\left(\frac{1}{\chi_-^2}+\frac{1}{\chi_+^2}\right)+m_\pi^2\Delta_{s_1s_1}\right\},\\
R_{\pi\pi} &= |F_\pi(s)|^2\left\{A\frac{4s_1}{\chi'_-\chi'_+}-\frac{8m_\pi^2}{s^2}\left(\frac{tu_1}{\chi'^2_+}+\frac{t_1u}{\chi'^2_-}\right)+m_\pi^2\Delta_{ss}\right\},\\
R_{e\pi} &= \Re\mathrm{e}(F_\pi(s)F_\pi^*(s_1))\left\{4A\left(\frac{u}{\chi_-\chi'_+}+\frac{u_1}{\chi_+\chi'_-}\right.\right.\\
&\left.\left.-\frac{t}{\chi_-\chi'_-}-\frac{t_1}{\chi_+\chi'_+}\right)+m_\pi^2\Delta_{ss_1}\right\},
\end{aligned}
$$

$$
\begin{aligned}
A &= \frac{tu+t_1u_1}{ss_1}\,, \quad \Delta_{s_1s_1} = -\frac{4}{s_1^2}\,\frac{(t+u)^2+(t_1+u_1)^2}{\chi_+\chi_-}\,,\\
\Delta_{ss} &= \frac{2m_\pi^2(s-s_1)^2}{s(\chi'_-\chi'_+)^2} + \frac{8}{s^2}(tt_1+uu_1-s^2-ss_1),\\
\Delta_{ss_1} &= \frac{8}{ss_1}\Bigg[\frac{2(t_1-u)+u_1-t}{\chi'_-} + \frac{2(t-u_1)+u-t_1}{\chi'_+}\\
&\quad + \frac{u_1+t_1-s}{2\chi_-}\left(\frac{u}{\chi'_+}-\frac{t}{\chi'_-}\right) + \frac{u+t-s}{2\chi_+}\left(\frac{u_1}{\chi'_-}-\frac{t_1}{\chi'_+}\right)\Bigg].
\end{aligned}
$$

The Mandelstam variables and $\chi_\pm, \chi'_\pm$ are defined as: $s=4\varepsilon^2,\ s_1=2p_1p_2,\ t=-2p_-p_1,\ t_1=-2p_+p_2,\ u=-2p_-p_2,\ u_1=-2p_+p_1,\ \chi_\pm=kp_\pm$ and $\chi'_\pm=kp_{1,2}$.

The same approach (as for muons) was applied to construct the *master* formula and to implement the *compensators* into it. When the *compensators* are added the cross section dependence on the both auxiliary parameters θ_0 and Δ disappears. The final expression describing production of pion pairs (*master* formula) reads

$$
\begin{aligned}
&\frac{\mathrm{d}\sigma^{e^+e^-\to\pi^+\pi^-(n\gamma)}}{\mathrm{d}\Omega_1} =\\
&= \int\limits_0^1\int\limits_0^1 \mathrm{d}x_1\mathrm{d}x_2\mathcal{D}(z_1,s)\mathcal{D}(z_2,s)\frac{\mathrm{d}\tilde\sigma_0(z_1,z_2)}{\mathrm{d}\Omega_1}\big(1+\frac{2\alpha}{\pi}\tilde K\big)\Theta(\text{cuts})\\
&+\frac{\alpha}{\pi}\int\limits_\Delta^1\frac{\mathrm{d}x_1}{x_1}\left[\big(z_1+\frac{x_1^2}{2}\big)\ln\frac{\theta_0^2}{4}+\frac{x_1^2}{2}\right]\frac{\mathrm{d}\tilde\sigma_0(z_1,1)}{\mathrm{d}\Omega_1}\Theta(\text{cuts})\\
&+\frac{\alpha}{\pi}\int\limits_\Delta^1\frac{\mathrm{d}x_2}{x_2}\left[\big(z_2+\frac{x_2^2}{2}\big)\ln\frac{\theta_0^2}{4}+\frac{x_2^2}{2}\right]\frac{\mathrm{d}\tilde\sigma_0(1,z_2)}{\mathrm{d}\Omega_1}\Theta(\text{cuts})\\
&+\frac{\alpha^3}{32\pi^2 s}\int\limits_{\substack{k^0>\Delta\varepsilon\\ \theta_\gamma>\theta_0}} R_{\mathrm{hard}}^{e^+e^-\to\pi^+\pi^-\gamma}\frac{\mathrm{d}\Gamma}{\mathrm{d}\Omega_1}\Theta(\text{cuts})\\
&+\frac{2\alpha}{\pi}\left[\frac{1+\beta^2}{2\beta}\ln\frac{1+\beta}{1-\beta}-1+2\ln\frac{1-\beta c_1}{1+\beta c_1}\right]\ln\frac{\Delta\varepsilon}{\varepsilon}\cdot\frac{\mathrm{d}\tilde\sigma_0(1,1)}{\mathrm{d}\Omega_1}, \quad (54)
\end{aligned}
$$

where $\tilde K=\pi^2/6-1/4+K^\pi_{\mathrm{even}}(\tilde s,\tilde\theta_1)+K^\pi_{\mathrm{odd}}(\tilde s,\tilde\theta_1)$, $\tilde\theta_1$ is a negative pion polar angle in center-of-mass system; $\Theta(\text{cuts})$ is a theta-function with the kinematic

restrictions applied to pions by selection criteria. The above formula consists of the following parts:

- the cross section with emission of jets collinear to the the beam axis with two *compensators*;
- the cross section with one hard photon emission outside the narrow cones was derived in the first order of α exactly keeping the all terms proportional to m_π^2/s;
- the cross section with soft and virtual photon emission by the initial and final particles;
- non-leading terms proportional to the Born cross section are taken into account by means so-call *K-factor*.

To simulate the events of the process $e^+e^- \to \pi^+\pi^- + n\gamma$ and to calculate the cross section numerically, the integration limits with energy in the first term in Eq. (54) were again divided in two parts from 0 to $\Delta\varepsilon$ and from $\Delta\varepsilon$ to the maximal jet energy. As a result, the two-fold integral splits into four separate integrals. Those of them which describe one jet radiation are combined by a proper way with the *compensators* in the *master* formula. The contribution due to soft and virtual corrections together with the Born cross section reads

$$\frac{\mathrm{d}\sigma_1^{e^+e^-\to\pi^+\pi^-(n\gamma)}}{\mathrm{d}\Omega_1} = \int\limits_0^\Delta\int\limits_0^\Delta \mathrm{d}x_1\mathrm{d}x_2\mathcal{D}(z_1,s)\mathcal{D}(z_2,s)\big(1+\frac{2\alpha}{\pi}\tilde{K}\big)\frac{\mathrm{d}\tilde{\sigma}_0(z_1,z_2)}{\mathrm{d}\Omega_1}$$
$$+\frac{2\alpha}{\pi}\left[\frac{1+\beta^2}{2\beta}\ln\frac{1+\beta}{1-\beta}-1+2\ln\frac{1-\beta c_1}{1+\beta c_1}\right]\ln\frac{\Delta\varepsilon}{\varepsilon}\frac{\mathrm{d}\tilde{\sigma}_0(1,1)}{\mathrm{d}\Omega_1}\,. \qquad (55)$$

The cross section with a hard jet emission along the electron momentum (with the condition that one hard photon is inside the narrow cone) reads

$$\frac{\mathrm{d}\sigma_2^{e^+e^-\to\pi^+\pi^-+n\gamma}}{\mathrm{d}\Omega_1} = \int\limits_\Delta^1\int\limits_0^\Delta \mathrm{d}x_1\mathrm{d}x_2\mathcal{D}(z_2,s)\Big[\mathcal{D}(z_1,s)\big(1+\frac{2\alpha}{\pi}\tilde{K}\big)$$
$$+\frac{\alpha}{\pi}\frac{1}{x_1}\left(\big(z_1+\frac{x_1^2}{2}\big)\ln\frac{\theta_0^2}{4}+\frac{x_1^2}{2}\right)\Big]\frac{\mathrm{d}\tilde{\sigma}_0(z_1,z_2)}{\mathrm{d}\Omega_1}\Theta(\text{cuts}). \qquad (56)$$

The analogous contribution with one jet along the positron momentum is

given by

$$\frac{\mathrm{d}\sigma_3^{e^+e^-\to\pi^+\pi^-+n\gamma}}{\mathrm{d}\Omega_1} = \int\limits_0^{\Delta}\int\limits_{\Delta}^{1} \mathrm{d}x_1\mathrm{d}x_2\mathcal{D}(z_1,s)\Big[\mathcal{D}(z_2,s)\big(1+\frac{2\alpha}{\pi}\tilde{K}\big)$$
$$+\frac{\alpha}{\pi}\frac{1}{x_2}\bigg(\big(z_2+\frac{x_2^2}{2}\big)\ln\frac{\theta_0^2}{4}+\frac{x_2^2}{2}\bigg)\Big]\frac{\mathrm{d}\tilde{\sigma}_0(z_1,z_2)}{\mathrm{d}\Omega_1}\Theta(\text{cuts}). \qquad (57)$$

The cross section with two jets along motion of the initial particles is described by

$$\frac{\mathrm{d}\sigma_4^{e^+e^-\to\pi^+\pi^-+n\gamma}}{\mathrm{d}\Omega_1} =$$
$$= \int\limits_{\Delta}^{1}\int\limits_{\Delta}^{1} \mathrm{d}x_1\mathrm{d}x_2\mathcal{D}(z_1,s)\mathcal{D}(z_2,s)\big(1+\frac{2\alpha}{\pi}\tilde{K}\big)\frac{\mathrm{d}\tilde{\sigma}_0(z_1,z_2)}{\mathrm{d}\Omega_1}\Theta(\text{cuts}). \qquad (58)$$

Emission of a single hard photon outside the narrow cones is given by

$$\frac{\mathrm{d}\sigma_5^{e^+e^-\to\pi^+\pi^-+\gamma}}{\mathrm{d}\Omega_1} = \frac{\alpha^3}{32\pi^2 s}\int\limits_{\substack{k^0>\Delta\varepsilon\\ \theta_\gamma>\theta_0}} R_{\text{hard}}^{e^+e^-\to\pi^+\pi^-\gamma}\frac{\mathrm{d}\Gamma}{\mathrm{d}\Omega_1}\Theta(\text{cuts}). \qquad (59)$$

Numerical tests have been done for the c.m.s. energy of 900 MeV. Figs. 18, 19 show the cancellation of cross section dependence on the auxiliary parameters $\Delta\varepsilon$ and θ_0 in the broad range of its values. The cross section variations are inside the corridor with the width about $\sim 0.1\%$.

A comparison with the BABAYAGA [20] generator was performed. The theoretical accuracy of the formulae, used in BABAYAGA program, is about 1%. BABAYAGA code doesn't include the photon emission by pions. Therefore this term was removed from our code (just for comparisons). The difference of the cross sections calculated by MCGPJ generator and BABAYAGA is shown in Fig. 20 with the same selection criteria as for events of Bhabha scattering. A systematic shift between cross sections is seen at the $\sim 1\%$ level in conformity with the BABAYAGA code precision. The observable difference is explained by the different fit functions which are used for the cross section approximation. The distributions produced by both generators have very similar shapes as close as it was for muons with the precise KKMC event generator. It can serve as an indirect confirmation that some constant term was missed in formulae for the BABAYAGA code (it is only our assumption).

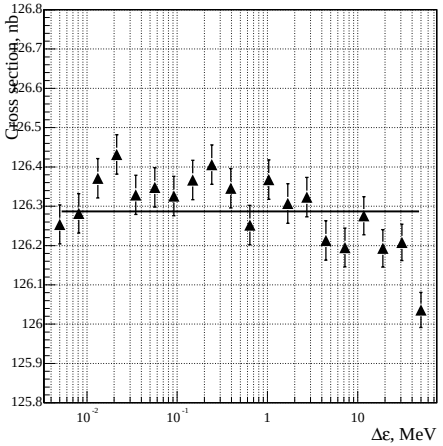

Figure 18: Dependence of the $\pi^+\pi^-$ cross section on the auxiliary parameter $\Delta\varepsilon$.

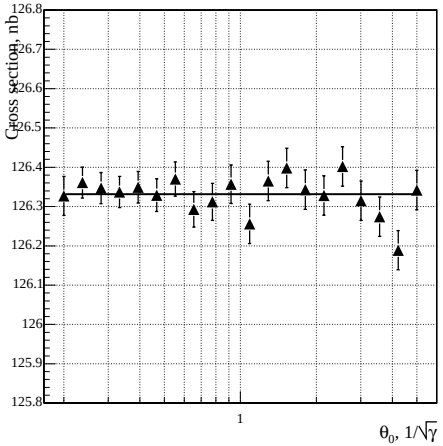

Figure 19: Dependence of the $\pi^+\pi^-$ cross section on the auxiliary parameter θ_0.

The distributions with the average momentum of pion, muon and electron pairs are presented in Fig. 21 at the c.m.s. energy of 390 MeV for experimental and simulated events. The number of simulated events exceeds the experimental one at least by a factor of one hundred. The momentum and angle resolutions, decays in flight, interaction with the detector matter and many other factors were *smeared* with the simulated events parameters to cre-

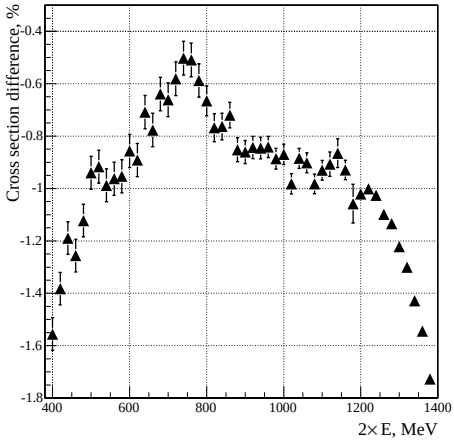

Figure 20: The relative difference between cross sections calculated by MCGPJ and BABAYAGA *versus* the c.m.s. energy.

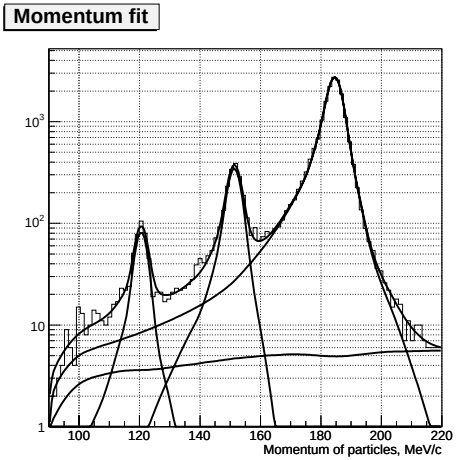

Figure 21: Distributions of pion, muon and electron pairs as a function of average momentum. The left, middle and right peaks corespond to $\pi/\mu/e$ events. The upper curve represents a common fit, bottom curve - background.

ate the events as close as possible the *real* ones. The histograms for each type of particles were fitted by two Gaussian functions. Their relative weights and

widths were free parameters under the fit. Good agreement between experiment and simulation is seen. It follows that the assumption about point-like pions is a reasonable approximation.

The enveloping curve, extracted from the fit, allows to describe the shape of the all three histograms at the *peaks* as well as at the *tails*. It permits to determine the number of events inside each histogram and to estimate the number of muon and electron events under the pion peak and thereby to extract the systematic error dealing with the procedure of events separation.

It is worth noting that the shape of the histogram tops of the simulated events is not described well, if the MC generator, based on the formulae in the first order in α, is used. The shape of the histogram tops is mainly driven by the soft photon emission spectrum and the apparatus resolution. The fit parameters are kept by the peaks shape where the main statistics are collected. Thus the number of events in the *tail* area is defined by the shape of the peaks. Hence, the approach with photon jets emission is absolutely necessary.

The MC generator simulating production of charged kaons in the reaction,

$$e^-(z_1 p_-) + e^+(z_2 p_+) \to K^-(p_1) + K^+(p_2),$$

is created in the same way as for pions. The pion mass m_π must be replaced in the above expressions by the mass of charged kaon and the Coulomb interaction in the final state near the threshold production should be taken into account by the common Sakharov-Zommerfeld factor [7]:

$$f(z) = \frac{z}{1-\exp(-z)} - z/2, \qquad z = \frac{2\pi\alpha}{v}$$
$$v = 2\sqrt{\frac{s-4m_K^2}{s}}\left(1+\frac{s-4m_K^2}{s}\right)^{-1}, \tag{60}$$

where v is the relative velosity of kaons. The term $z/2$ is subtracted from this factor since it is already included in the $\mathcal{O}(\alpha)$ RC to the final state. In addition, the pion form factor must be replaced by the corresponding one for kaons.

The MC generator simulating neutral kaons production in the reaction,

$$e^-(z_1 p_-) + e^+(z_2 p_+) \to K_L(p_1) + K_S(p_2),$$

is significantly simpler since there are no Coulomb interaction and photons emission in the final state. The *shifted* Born cross section has the same

analytic form like for charged kaons. The *master* formula for neutral kaons production, according to the given above, reads

$$\frac{\mathrm{d}\sigma^{e^+e^-\to K_L K_S(n\gamma)}}{\mathrm{d}\Omega_1} =$$
$$= \int\limits_0^1\int\limits_0^1 \mathrm{d}x_1\mathrm{d}x_2\mathcal{D}(z_1,s)\mathcal{D}(z_2,s)\frac{\mathrm{d}\tilde{\sigma}_0(z_1,z_2)}{\mathrm{d}\Omega_1}\big(1+\frac{2\alpha}{\pi}\tilde{K}\big)\Theta(\mathrm{cuts})$$
$$+\frac{\alpha}{\pi}\int\limits_\Delta^1 \frac{\mathrm{d}x_1}{x_1}\left[\big(z_1+\frac{x_1^2}{2}\big)\ln\frac{\theta_0^2}{4}+\frac{x_1^2}{2}\right]\frac{\mathrm{d}\tilde{\sigma}_0(z_1,1)}{\mathrm{d}\Omega_1}\Theta(\mathrm{cuts})$$
$$+\frac{\alpha}{\pi}\int\limits_\Delta^1 \frac{\mathrm{d}x_2}{x_2}\left[\big(z_2+\frac{x_2^2}{2}\big)\ln\frac{\theta_0^2}{4}+\frac{x_2^2}{2}\right]\frac{\mathrm{d}\tilde{\sigma}_0(1,z_2)}{\mathrm{d}\Omega_1}\Theta(\mathrm{cuts})$$
$$+\frac{\alpha^3}{32\pi^2 s}\int\limits_{\substack{k^0>\Delta\varepsilon\\ \theta_\gamma>\theta_0}} R_{\mathrm{hard}}^{e^+e^-\to K_L K_S(\gamma)}\frac{\mathrm{d}\Gamma}{\mathrm{d}\Omega_1}\Theta(\mathrm{cuts}), \qquad (61)$$

where $\tilde{K}=\pi^2/6-1/4$, $\Theta(\mathrm{cuts})$ imposes the relevant kinematic (and experimental) cuts, $R_{\mathrm{hard}}^{e^+e^-\to K_L K_S(\gamma)}$ consists of the one term which describes initial state radiation only.

5 Conclusion

MC generator to simulate the processes $e^+e^-\to e^+e^-$, $\mu^+\mu^-$, $\pi^+\pi^-$, K^+K^- and K_LK_S in the low energy range is described in ditail. An extended treatment of radiative corrections is implemented in the generator to get a high level of theoretical precision. The soft and virtual photons radiation is taken into account in the first order of α exactly as well as one hard photon emission outside of narrow cones. All terms in the matrix elements which are proportional to the muon or pion mass squared are kept. By means the SF formalism dealing with radiation of photon jets in the collinear region (so-called enhanced contributions) are included in the current version of the program - Monte Carlo Generator Photon Jets. As a result, the theoretical accuracy of the approach is estimated to be at 0.2%. It is better at least by a factor of two compared with the accuracy $0.5-1\%$ achieved in the earlier works. Comparison with the well known codes, BHWIDE and KKMC, showed good agreement for many distributions simulated by the generators.

The event distributions with given acollinearity angles $\Delta\theta$ and $\Delta\phi$ show good agreement with CMD-2 experimental data. The double ratio of the number of muon events to that of electrons divided on the ratio of the theoretical cross sections was found to be 0.986 ± 0.014. The deviation from unit is $-1.4 \pm 1.4\%$. Unfortunately the scare experimental statistics in this energy range does not allow to check the theoretical approach accuracy applied here with better precision. It is the first direct comparison of the experimental data with the theoretical calculation at the accuracy about $\sim 1\%$ level. The comparison of the momenta distributions in the lowest energy point showed that simulation with photon jets radiation describes the experimental spectra pretty well.

The theoretical uncertainties of the cross sections with RC are defined by the unaccounted higher order corrections and are estimated to be at 0.2% level. Let us list the main sources of uncertainties in the current formulae:

- The weak interaction contributions are omitted in our approach. The numerical estimations show that for energies $2\varepsilon < 10$ GeV these contributions do not exceed 0.1%.

- We omitted a part of the second order next-to-leading radiative corrections proportional to $(\alpha/\pi)^2 L \sim 10^{-4}$. Among these contributions we have: the effect due to double photon emission (one inside the narrow cones and one outside them); soft or virtual photon emission simultaneously with one hard photon emission, and so on. Even if we assume that a coefficient in front of these terms will be of the order of ten, their contribution can not exceed 0.1%.

- The third source of uncertainty is related with the calculation of the hadronic vacuum polarization contribution to the virtual photon propagator. Numerical estimations show that the systematic error of hadronic cross sections in 1% changes the leptonic cross section about $\sim 0.04\%$.

- The fourth source of uncertainty about 0.1% is related with the models which are used to describe the energy dependence of the hadronic cross sections.

- The last source of uncertainty is mainly driven by the collinear kinematics approximation - several terms proportional to $(\alpha/\pi)\theta_0^2$ and to $(\alpha/\pi)(1/\gamma\theta_0)^2$ were omitted. Indeed the photons inside jets have an angular distribution. Numerical evaluations show that a contribution of these factors is about $\sim 0.1\%$.

Considering the uncertainty sources mentioned above as independent, we can conclude that the total systematic error of the cross sections with RC is less than 0.2%. An indirect confirmation of the correct evaluation of the accuracy is the cross sections comparison with RC calculated in the first order of α only. The corresponding difference does not exceed 0.2%. It follows that the higher orders enhanced contributions, coming from collinear regions with emission of two and more photons, contribute to the cross section only $\sim 0.2\%$ for our selection criteria. Since the accuracy of this contribution is certainly known better than 100%, therefore the systematic theoretical error for the cross sections with RC is better than 0.2%.

The authors are grateful to all members of the CMD-2 collaboration, personally to V.S. Fadin and A.V. Bogdan, A.I. Milstein and G.N. Shestakov, S.I.Eidelman, I.B. Logashenko and B.I.Khazin for fruitful and useful discussions. We also are grateful to S. Jadach and W. Placzek for the help to run BHWIDE and KKMC code, G. Montagna and C.M. Carloni Calame for the useful collaboration in questions about BABAYGA code for events of Bhabha scattering.

This work is supported in part by the grants: RFBR-99-02-17053, RFBR-99-02-17119, RFBR-03-02-17077 and INTAS 96-0624.

References

[1] G.V. Bennett *et al.*, Phys. Rev. Lett. **89** (2002) 101804;
Erratum-ibid. **89** (2002) 129903.

[2] R.R. Akhmetshin *et al.*, Phys. Lett. B **89** (2002) 161;
R.R. Akhmetshin *et al.*, Nucl. Phys. B (Proc. Suppl.)**131** (2003) 3.

[3] S. Eidelman, F. Jegerlehner, Z. Physik C **67** (1995) 585;
M. Davier *et al.*, Eur. Phys. J. C **27** (2003) 497;
M. Davier, Nucl. Phys. B (Proc. Suppl.)**131** (2003) 192;
T. Teubner, Nucl. Phys. B (Proc. Suppl.)**131** (2003) 201.

[4] B. Lautrup, A. Peterman and E. de Rafael, Phys. Rep. **3** (1972) 193.

[5] (g-2) Collabaration, Proposal E969, BNL (2004).

[6] A.B. Arbuzov *et al.*, JHEP **10** (1997) 001.

[7] A.B. Arbuzov *et al.*, JHEP **10** (1997) 006.

[8] Z. Jakubowski *et al.*, Z. Phys. C **40** (1988) 49;
Y.S. Tsay, SLAC - PUB - 1515 (1973).

[9] E.A. Kuraev and V.S. Fadin, Sov. J. Nucl. Phys. **41** (1985) 466;
M. Cacciari, A. Deandrea and O. Nicrosini, Europhys. Lett. **17** (1992) 123;
A.B. Arbuzov *et al.*, JETP **81** (1995) 638;
A.B. Arbuzov *et al.*, Nucl. Phys. B **485** (1997) 457;
S. Yadach, M. Skrzypek and B.F.L. Ward, Phys.Lett. B **257** (1991) 173;
M. Skrzypek, Acta Phys. Polon, B **23** (1992) 135.

[10] F.A. Berends *et al.*, Nucl. Phys. B **122** (1977) 485;
F.A. Berends and R. Kleiss, Nucl. Phys. B **177** (1981) 237;
F.A. Berends, K.J.F Gaemers and R. Gastmans, Nucl. Phys. B **68** (1974) 541;
F.A. Berends and R. Kleiss, Nucl. Phys. B **228** (1983) 537;
S.I. Eidelman and E.A Kuraev, Phys. Lett. B **80** (1978) 94.

[11] V.N. Bayer, V.S. Fadin, V.A. Khoze, Nucl. Phys. B **65** (1973) 381.

[12] S. Jadach, W. Placzek, B.F.L. Ward, Phys. Lett. B **390** (1997) 298.

[13] I.B. Khriplovich, Sov. J. Yad. Fiz, **17** (1973) 576;
D.A. Dicus, Phys. Rev. D **8** (1973) 890.

[14] S.I. Eidelman, E.A. Kuraev, V.S. Panin, Nucl. Phys. B **148** (1979) 245;
F.A. Berends, R. Kleiss, P. De Causmaecker, R. Gastmans, and T.T. Wu, Phys. Lett. B **103**, 124 (1981).

[15] E.A. Kuraev, G.V. Meledin, Nucl. Phys. B **122** (1977) 485.

[16] S. Jadach *et al.*, Comp. Phys. Commun. **130** (2000) 260.

[17] R.W. Brown and K.O. Mikaelian, Lett. Nuovo Cim. **10** (1974) 305.

[18] A. Hoefer, J. Gluza and F. Jegerlehner, Eur. Phys. J. C **24** (2002) 51.

[19] V.N. Bayer, VIII Winter School LINP, v.II (1973) 164;
O.P. Sushkov, Sov. J. Yad. Fiz. **22** (1975) 868.

[20] C.M. Carloni Calame et al., Nucl. Phys **B584** (2000) 459;
C.M. Carloni Calame, Phys. Lett. **B520** (2001) 16.

A.B. Arbuzov, G.V. Fedotovich, F.V. Ignatov,
E.A. Kuraev, A.L. Sibidanov

Monte-Carlo generator for the processes $e^+e^- \to e^+e^-$, $\mu^+\mu^-$, $\pi^+\pi^-$ and K^+K^-, K_LK_S with precise radiative corrections at low energies

А.Б. Арбузов, Г.В. Федотович, Ф.В. Игнатов,
Е.А. Кураев, А.Л. Сибиданов

Монте-Карло генератор процессов $e^+e^- \to e^+e^-$, $\mu^+\mu^-$, $\pi^+\pi^-$ и K^+K^-, K_LK_S с прецизионными радиационными поправками при низких энергиях

Budker INP 2004-70

Ответственный за выпуск А.М. Кудрявцев
Работа поступила 23.11.2004 г.

Сдано в набор 26.11.2004 г.
Подписано в печать 30.12.2004 г.
Формат бумаги 60×90 1/16 Объем 2.9 печ.л., 2.3 уч.-изд.л.
Тираж 100 экз. Бесплатно. Заказ № 70

Обработано на IBM PC и отпечатано на
ротапринте ИЯФ им. Г.И. Будкера СО РАН
Новосибирск, 630090, пр. академика Лаврентьева, 11.